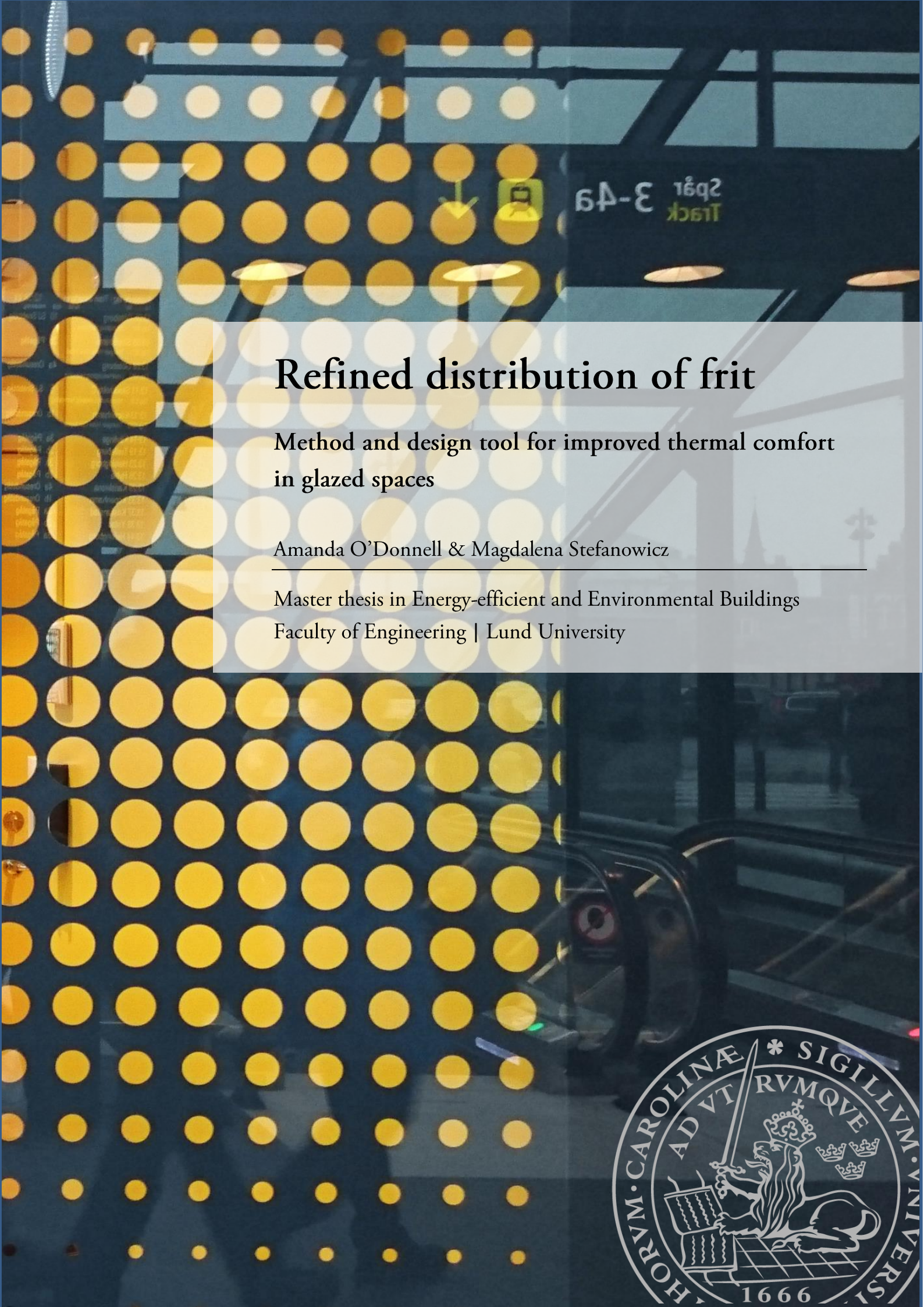

Refined distribution of frit

Method and design tool for improved thermal comfort in glazed spaces

Amanda O'Donnell & Magdalena Stefanowicz

Master thesis in Energy-efficient and Environmental Buildings
Faculty of Engineering | Lund University

Lund University

Lund University, with eight faculties and a number of research centers and specialized institutes, is the largest establishment for research and higher education in Scandinavia. The main part of the University is situated in the small city of Lund which has about 112 000 inhabitants. A number of departments for research and education are, however, located in Malmö. Lund University was founded in 1666 and has today a total staff of 6 000 employees and 47 000 students attending 280 degree programmes and 2 300 subject courses offered by 63 departments.

Master Programme in Energy-efficient and Environmental Building Design

This international programme provides knowledge, skills and competencies within the area of energy-efficient and environmental building design in cold climates. The goal is to train highly skilled professionals, who will significantly contribute to and influence the design, building or renovation of energy-efficient buildings, taking into consideration the architecture and environment, the inhabitants' behavior and needs, their health and comfort as well as the overall economy.

The degree project is the final part of the master programme leading to a Master of Science (120 credits) in Energy-efficient and Environmental Buildings (EEBD).

Keywords: Thermal comfort, glazed spaces, *g*-value, overheating, solar shading, frit, parametric design

Abstract

Thermal comfort in highly glazed spaces has long proven to be a troublesome matter due to unwanted passive solar heat gains and consequent elevated cooling loads.

A methodology has been developed to correlate overheating in glazed spaces with shading need. Outcomes of the method are indicative of regions of a façade which are subject to problematic solar gains. A particular distribution of shading is suggested in order to mitigate thermal discomfort as a result of the identified problematic gains. A light, reflective ceramic shading device, known as frit, has been utilized to selectively adjust solar heat transmission, namely *g*-value, through glazing. The methodology was further developed into a design tool, scripted in Rhino/Grasshopper, facilitating parametric applicability.

Results of shading distribution according to the method indicate that the design tool is successful in reducing local peak temperatures in a glazed office space (for Swedish climate conditions), achieving up to 9%, 19%, 32% and 87% annual reduction of hours where temperatures exceed 26°C, 28°C, 30°C and 35°C respectively. Other results include; the tool being most efficient for local overheating problems, decreasing coherently with increased analysis area. Further, the usability of the tool increases notably with reasonable initial overheating problems, indicating that the tool could be a beneficial complement to a functioning ventilation system, rather than a substitute. Moreover, by concentrating shading where it is needed most, the average *g*-value of the whole façade can be increased with as much a 11%, whilst still maintaining initial number of hours above 35°C, showing potential for the method/tool to contribute to economic and environmental savings for highly glazed spaces in Sweden.

These outcomes prove favorable for further development of the methodology to decipher more complex building geometries and user specifications.

Acknowledgements

We would like to thank our supervisor Henrik Davidsson for his rational guidance and selfless support. We would have lost track many times without you. Immense gratitude goes to our mentor Harris Poirazis for his knowledge, encouragement and passion for the project, pushing us and the project beyond our expectations. Further, we would like to thank the Hans Eliasson Foundation for supporting the EEBD Master programme.

Contribution

The project has inherently been a collaborative process and was developed with equal contribution of Amanda and Magdalena. The methodology was consequentially planned and processed in great detail by both authors. Tool definitions were collectively structured throughout. With regard to scripting, Amanda focused more on thermal module and data module of the tool and Magdalena worked more on solving the ray tracing module. All encountered problems in the scripting were solved together and the definitions were continuously refined in accordance with ambitions of both authors. All output from the separate modules of the tool was analyzed by both parts, with comparative and critical reasoning.

Interpretation of numerical data and translation to graphical results were developed together. Visual communication of results were mainly shaped by Magdalena where as written output was mainly articulated by Amanda, with continuous feedback from both parts.

Table of content

Abbreviations

A_p - projected area of the body
A_{sh} – Total shading frit area need, m^2
A_{facade} – Total façade area, m^2
$A_{\Delta Tfactor}$ – Single frit area relative to ΔT *factor*
$A_{sh,unit}$ – Shading area needed for a glazing unit, m^2
A_{unit} – Area of a glazed unit, m^2
A_{frit} - Area of a single frit dot, m^2
$A_{frit,unit}$ – Total frit area needed for a glazing unit, m^2
A_D - the DuBois surface area of the assumed person (ca. 1.8 m2)
α_{SW} - short-wave absorptivity (0.67 for white skin and average clothing)
α_{LW} - lon*g*-wave emissivity/absorptivity, typically equal to 0.95
DGU – double glazing unit
E_R – Solar heat energy reflected to the outside
E_{DT} – Direct solar heat energy transmitted to the inside
E_A – Solar heat energy absorbed by the glazing
E_{AT} – fraction of energy absorbed by the glazing and transferred to the inside
ERF – effective radiant field
.epw – EnergyPlus weather file format
f_{eff} - fraction of the body surface exposed to radiation from the environment (0.696 for a seated person)
f_{svv} - fraction of sky vault in occupant's view
f_{bes} - fraction of body exposed to sun
g-value – shading coefficient
g_{av} - average *g*-value
$g_{non\text{-}shaded}$ – non-shaded glass *g*-value
GH – Grasshopper, a graphical algorithm editor
HB and LB - Honeybee and Ladybug, open source environmental plugin for Grasshopper
HOY – hour of year, 8760 hours each year
h_r - radiation heat transfer coefficient (W/m^2 K)
I_{diff} - diffuse sky irradiance received on an upward-facing horizontal surface (W/m2)
I_{TH} - total outdoor solar radiation on the horizontal plane (W/m2)
I_{dir} – direct beam (normal) solar radiation (W/m2)
Low-e – low emissivity
MRT – mean radiant temperature (°C)
MRT_{Adj} – mean radiant temperature adjusted to compensate for the effect of short wave solar radiation on *U*-value - rate of heat transfer (W/m^2 K)
R_{floor} - reflectance of the floor
T_o – operative temperature (°C)
$T_{op,Adj}$ – solar adjusted operative temperature (°C)
T_{air} – air temperature (°C)
T_{sol} – total solar transmittance of a window system
TR_{sh} – Frit transparency
VT - visual transmittance

1 Introduction

The energy required to heat and cool our buildings, and the very way we define the "comfortable" thermal conditions we are trying to maintain, play significant roles in this environmental impact [of buildings]. The use of energy for heating, ventilating and air-conditioning (HVAC) of the indoor environment is already the largest sector in energy consumption in most of the developed world. (de Dear & Brager & Cooper, 1997)

Thermal neutrality occurs when the body is in equilibrium with its surroundings. The stability of an indoor climate, enabling thermal neutrality, depends highly upon the thermal resistance of the building envelope, for which glazing is an Achilles heel.

Highly glazed envelopes are prominent in modern architecture for many reasons, including; increased levels of natural light, views to the exterior and, when desired, passive solar gains. However, when not desired, the consequences of passive solar gains on the indoor environment are considerable, for which many buildings must overcompensate with intensive mechanical cooling and additional shading in order to comply with building standards and comfort regulations.

Advanced glazing systems are often introduced as an all-encompassing shading mechanism of glazed facades, incorporating multiple layers of glass, gases and/or solar control coatings to lower the solar energy transmittance of glazing, namely the *g*-value. The complexity of these glazing solutions, however, tend to subside architects' original ambitions of transparency, becoming particularly apparent in, for example, multifunctional glazed spaces, where daylight and views may be desired in some places, but in others, not.

Hereby, the purpose of this study was to develop a method, aiming to correlate specified overheating problems with customized shading need of glazed facades. The method is depicted in a parametric design tool, which identifies regions of a façade source to critical thermal discomfort indoors and hereafter suggest means of distributing the *g*-value of the façade, in order to lessen these problems locally.

1.1 Problem motivation

A need was expressed by the industry to innovatively connect overheating in glazed spaces with customized shading solutions for quick and informed decision making in the early design phase. To challenge conventional procedure by investigating a parametric approach to shading design was an appealing notion which inspired the thesis.

1.2 Objectives and aims

The primary objective was to create a comprehensive methodology able to identify regions on a façade experiencing solar gains which result in thermal discomfort for occupants. Secondly, to investigate to what extent thermal discomfort can be lessened by eliminating solar radiation falling directly on occupants. Thirdly, to depict the methodology in a design tool. The tool should provide suggestions for shading distribution as well as enable iterative processing of results and provide designers with knowledge to inform their design. The tool should be parametric, enabling applicability on a wide range of geometrical, geographical and behavioral cases.

1.3 Limitations

The method has been run on a simple "box" building geometry, representing a freestanding office with no furniture or obstructing geometries. The results of the method/tool are based on simulations only, for which the conformance to physical measurements is unknown. Regarding the simulation setup, a few limitation have been made. Firstly, the analysis of thermal comfort in the study is restricted to temperature parameters, i.e thermal comfort is measured in adjusted operative temperature. Any secondary effects of the method on other comfort parameter have been ignored. Secondly, construction materials and schedules from the simulation engine's built in database have been used, for which some deviation to Swedish standards may have occurred. Thirdly, no angular dependent properties of incident solar radiation have been considered. These simplifications are explained further in the Method section of the report.

2 State of the art

Initial analyses revealed that there is limited availability of multifunctional parametric tools relevant to this study on the market. With regards to shading design and solar adjusted thermal comfort, the following studies have been reviewed.

1. Shaderade

Sargent, Niemasz & Reinhart from Harvard University have developed a method; Shaderade, generating a three dimensional form of static shading based on indoor thermal comfort criteria. The method assesses optimal volumes of shading by projecting solar vectors from a window surface of a room onto a user-defined shading volume. The shading need is based on a balance of direct solar radiation contributing to overheating and available cooling capacity at each time interval during the analysis period. The cooling load is calculated with EnergyPlus.

The study comparatively concludes that the Shaderade form finding methodology for shading is more effective in cooling load reduction than many existing methods for static shading design (Sargent & Niemasz & Reinhart, 2011). This result indicates that ray-tracing shows potential as a means of identifying problematic solar gains.

2. SolarCal

Arens, Hoyt & Zhou discuss how the effect of direct solar radiation falling on the human body has not been considered in thermal comfort standards as of yet, highlighting how all thermal comfort predictions for occupants exposed to direct sunlight may be distorted. They developed a method; SolarCal, to calculate thermal comfort considering solar radiation falling on the human body. The calculation considers an increase in mean radiant temperature equivalent to shortwave heat gains from direct, diffuse, and indoor-reflected radiation based on additional radiant heat flux to or from the human body.

Comparison of results from SolarCal and physical measurements shows the SolarCal method achieves reasonable predictions of solar effects on mean radiant temperatures (Arens & Hoyt & Zhou, 2015). Calculation details of the SolarCal method is further explained in *Section 3.1.2.4 Adjusted mean radiant temperature (MRTAdj).*

3 Theory

This chapter includes theoretical aspects which have been considered when deriving the methodology.

3.1 Thermal comfort

Thermal comfort is defined as "*that state of mind which expresses satisfaction with the thermal environment"* (ANSI/ASHRAE Standard 55, 2010). Since a "state of mind" is a highly subjective, thermal comfort is a difficult matter to quantify. Nevertheless, there is a common understanding of that the thermal balance of the human body varies with a range of environmental and physical parameters.

The environmental parameters include air temperature, mean radiant temperature, relative air velocity and humidity. The physical parameters include metabolic heat production and clothing level (ISO, 2005).

3.1.1 Thermal comfort in glazed spaces

Understanding the influence of windows on thermal comfort is important not only to help designers create comfortable buildings, it will also help evaluate the benefits of improved windows. (Huizenga & Zhang & Mattelaer & Yu & Arens & Lyons, 2006, p. 5)

Heat is transferred to and from a space as a result of a temperature gradient between a surface e.g. a window and air in the space in three main ways:

1. conduction,
2. convection and
3. solar radiation

A highly glazed building envelope is more sensitive to convective losses to the outdoor environment than corresponding opaque facades (Poirazis, 2008). Despite advancement of high performance glazing technologies, glass remains a thermally deficient component of a building envelope. Hereby, glazing generates a more volatile and seasonally fluctuating indoor climate, often leading to increased cooling and heating loads. In winter, a window's effect on thermal discomfort depends mainly on insulative performance which refers to the heat transfer by conduction. The summer effect, however, depends on insulative performance as well as transmission of solar raditation (Poirazis, 2008).

3.1.1.1 Solar radiation

Glazing absorbs and transmits a significant amount of solar radiation. As shown in *Figure* 1, there are three ways in which glazing impacts thermal comfort (Huizenga & Zhang & Mattelaer & Yu & Arens & Lyons, 2006), namely:

1. short-wave radiation,
2. long-wave radiation and
3. induced air motion (convective drafts)

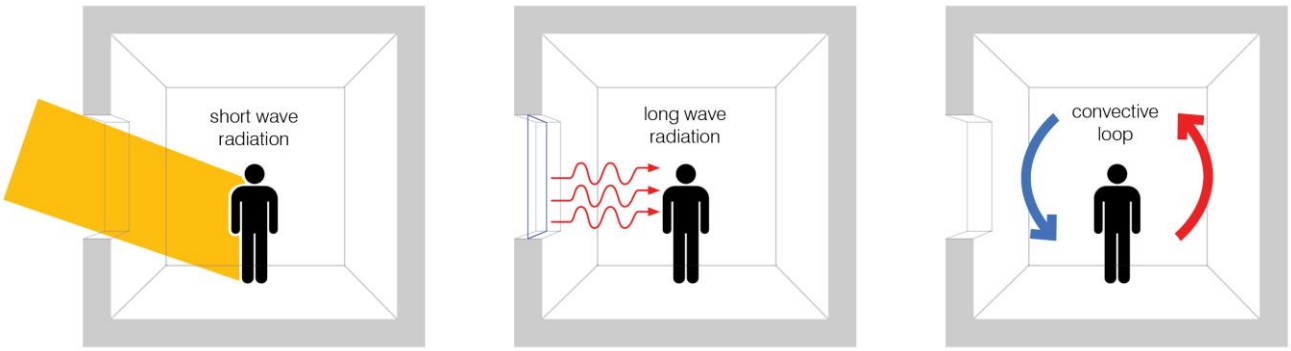

Figure 1: Window effect on thermal comfort

Short-wave radiation

Short-wave radiation is the transimited solar radiation through glazing, consisting of two components; direct and diffuse radiation.

The direct component is the radiation from the direct solar beam. When falling on an occupant, the direct component has the most significant impact on experienced thermal comfort (CIBSE, 2006), affecting the occupant in two ways; (1) directly when absorbed by the body and (2) indirectly by increasing the air and surface temperatures in the space (Huizenga & Zhang & Mattelaer & Yu & Arens & Lyons, 2006).

The diffuse component is the radiation which reaches the window after being scattered/reflected by clouds or air particles outside. The amount of sky covered in clouds is depicted as a fraction of total skype coverage on a scale from 0 to 10, where 0 is clear skies and 10 is total cloud coverage (Roudsari, 2015).

Long-wave radiation

Absorbed solar radiation increases the temperature of the glass. Consequently, lon*g*-wave radiation is emitted. Long-wave radiation refers to the radiant heat transfer from the warm or cold interior glass surface of a window, affecting an occupant's comfort in two ways; (1) It affects the body's comfort perception by influencing the overall radiative heat exchange between the body and the surrounding surfaces and (2) as the glazing becomes warmer than other indoor surfaces it creates radiant asymmetry. Hereby, the window acts as a radiator emitting additional heat to the room, which might become an additional source of discomfort (Huizenga & Zhang & Mattelaer & Yu & Arens & Lyons, 2006).

Apart from direct short-wave radiation falling on an occupant, lon*g*-wave radiation between the window and the rest of the room is the second most significant factor influencing thermal comfort (Lyons & Arasteh & Huizenga, 1999).

Convective drafts

Convective drafts are air motions induced by a difference between glass surface temperature and adjacent air temperature. Convective drafts occur when indoor air meets the cooler surface of glass and sinks towards the floor, creating a circular air movement. In winter, drafts often cause a local cooling of a body. In summer, however, the air motion may be desirable to stimulate natural ventilation in buildings (Huizenga & Zhang & Mattelaer & Yu & Arens & Lyons, 2006).

As the thermal comfort analyses in the thesis are restricted to temperature parameters, the effect of convective drafts have henceforth been ignored.

3.1.1.2 Optical properties of glazing

Solar heat gain through a window is dependent on two main components: transmitted and absorbed radiation. The transmitted radiation corresponds to how much short wave radiation reaches the occupant, while the absorbed radiation corresponds to how much a window temperature increases. (Huizenga & Zhang & Mattelaer & Yu & Arens & Lyons, 2006) Additionally, a certain fraction of solar radiation is being reflected from the glazed surface to the outside.

Relations between absorbed, reflected and transmitted radiation through a window are illustrated in *Figure 2* and described in Equation 1:

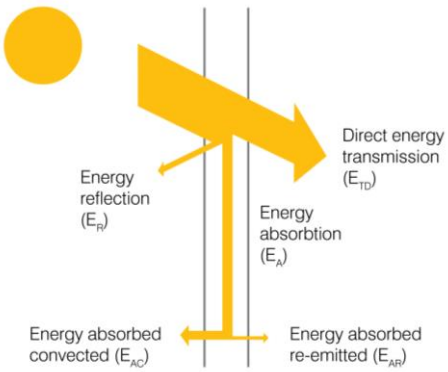

Figure 2: Solar heat energy transferred through a glazing.

$$E_R + E_{DT} + E_A = 1 \qquad \textit{Equation 1}$$

Where,
E_R – Solar heat energy reflected to the outside
E_{DT} – Direct solar heat energy transmitted to the inside
E_A – Solar heat energy absorbed by the glazing
E_C – Solar heat energy absorbed and reflected to the outside
E_{AR} – Fraction of energy absorbed by the glazing and transferred to the inside

3.1.1.2.1 Simple window indices

Three window indices are utilized for thermal calculations performed in this study (Griffith & Arasteh & Kohler, 2009):

1. *U*-value

The rate of heat transfer through a window measured in W/(m^2·K).

2. *g*-value

g-value (or Solar heat gain coefficient, SHGC) is a commonly used shading coefficient, representing the fraction of incident solar radiation transmitted by a window, where 1 represents maximum possible solar heat transmission, and 0 represents none. It is expressed as the sum of direct solar energy transmitted and the secondary internal heat transfer of energy absorbed in the glazing (Rosenfeld, 1996).

$$g\text{-value} = E_{DT} + E_{AR} \qquad \textit{Equation 2}$$

Where,
E_{DT} – Direct solar heat energy transmitted to the inside
E_{AR} – Fraction of energy absorbed by the glazing and transferred to the inside

When *g*-value alone is used to describe the solar radiation transmitted in building simulation, results are approximate. Standardized *g*-values (EN 410) are determined for normal incidence, whilst the angular properties of different types of glazing vary with number of layers and coatings (Standards, 2011). Consequently, two windows of the same *g*-value might have different ratios of transmitted and absorbed solar radiations (Griffith & Arasteh & Kohler, 2009).

3. Visible transmittance

The visual transmittance (*VT*) of a glazing is the amount of visible light which can pass through the glass. *VT* is influenced by glazing type, number of panes and any coatings.

3.1.1.3 Solar control of glazing

A common way of lowering *g*-value and thereby reducing the solar transmittance of a glazing, is to apply reflective coatings, which increases the glazing's reflectivity. High performance tinted glass and low-e coatings are able to provide *g*-value for a double glazed window between 0.2 and 0.7 and a light transmittance between 0.3 and 0.8 W/m^{2}K (Poirazis, 2008). However, when very low *g*-value glass is applied uniformly

across a façade, the light transmittance is likely to be insufficient and views to the outside might be disturbed with coating's coloring.

3.1.1.3.1 Fritted glass

An alternative solar control is fritted glass. Frit is the name of a static shading material, added to a surface of a glazing system often in a specified pattern, as shown in *Figure 3.* Applied pattern of ceramic frit can be either opaque or translucent. The solar-control effect depends on the ratio of clear glass to fritted area (Schittich & Sobek & Staib & Balkow & Schuler, 2007).

Various ceramic fritted glazing is available, to name a few:

- Single pane with ceramic frit on interior side
- Double pane with ceramic frit placed on interior side of outer pane
- Triple pane with ceramic frit on exterior side of middle pane

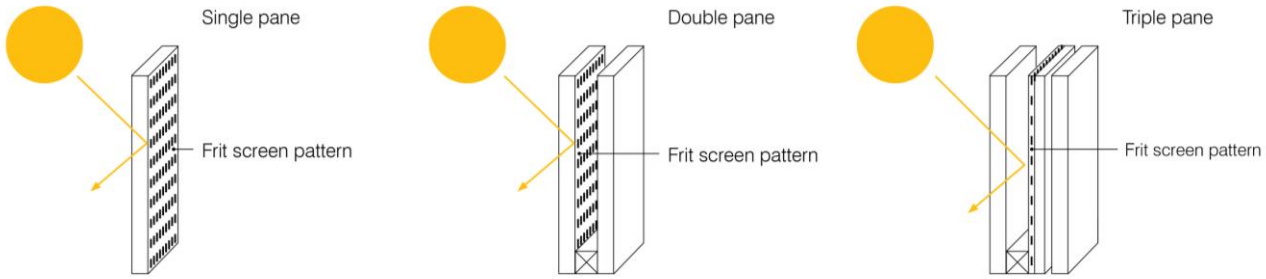

Figure 3: Frit glass assembly.

Further, fritted glass is available in various ranges of pattern as shown in *Figure 4,* with frit coverage up to 60%.

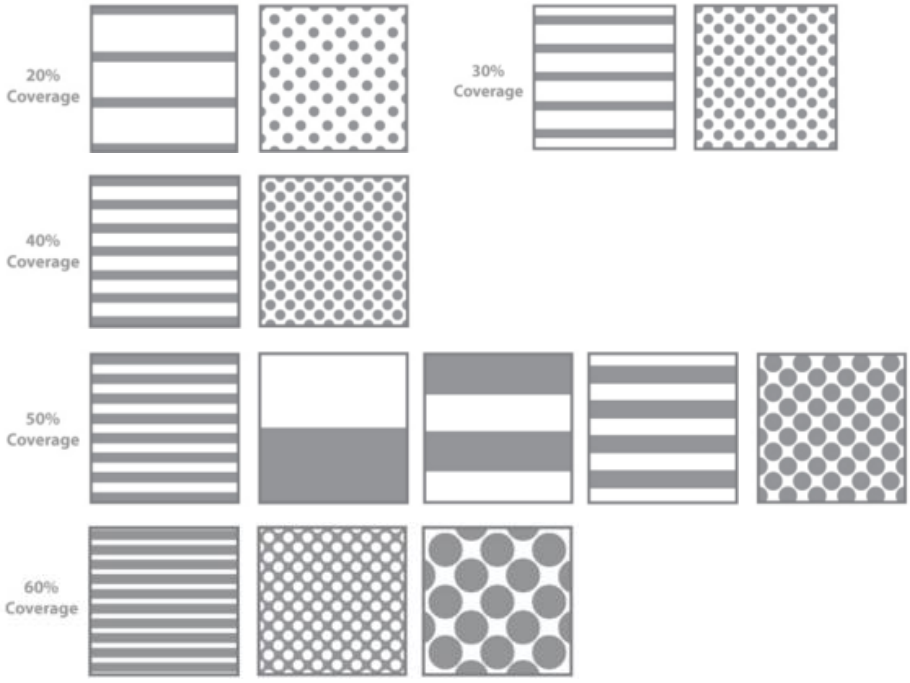

Figure 4: Silk-screen patterns.

3.1.1.3.2 Shading coefficient of fritted glass

Glazing unit is a commonly used term to describe an independent part of a window, usually separated with a frame. Glazing units may consists of specific types of glass and filling gases, for which separate units may have specific simple as explained in 3.1.1.2.1 Simple window indices.

For specific types of multi-layered glazing units with frit, *g*-value is commonly defined by producers or can be calculated in more complex ways, which include angle-dependent *g*-values or three-dimensional heat transfer calculations (Karlsson, 1999). For these calculations many specific optical properties of the glazing, often

difficult to obtain, are required. Hereby, for the purpose increasing the functionality of the method, a simplified average *g*-value calculation is utilized. The calculation, displayed in *Equation 3,* considers single pane glazing units with frit, where the total average *g*-value is defined as area-weighted sum of the individual area's *g*-values. (McCluney, 2002)

$$g_{av} = \frac{(g_1 * A_1) + (g_2 * A_2) + (g_3 * A_3) + (g_4 * A_4)}{A_1 + A_2 + A_3 + A_4}$$

Equation 3

Where,

A_1, A_2, A_3, A_4 – areas of individual glazing units
g_{av} – average *g*-value of a glazing
g_1, g_2, g_3, g_4 – *g*-values of individual glazing units

3.1.1.4 Glazing to floor ratio

Glazing to floor ratio, *GFR,* indicates how much a space is glazed with regards to its floor area. A minimum sufficient level of GFR for a low-energy office buildings in cold climate is considered to be 12%. (Persson, 2006)

3.1.2 Comfort temperature parameters

According to CIBSE (2006), temperature is usually the most important environmental parameter affecting thermal comfort in spaces. Comfort temperature parameters of air temperature, mean radiant temperature and operative temperature are described below.

3.1.2.1 Air temperature (T_{air})

Air temperature is the physical temperature of the air. Measurement points are exposed to the air but shielded from radiation and moisture.

3.1.2.2 Mean radiant temperature *(MRT)*

Mean radiant temperature represents an impact of long wave radiation, radiant heat, emitted from the surrounding surfaces.

3.1.2.3 Operative temperature (T_{op})

Operative temperature is the average of air temperature and radiant temperature experienced by an occupant and can be calculated according to *Equation 4:*

$$T_o = \frac{T_{air} + MRT}{2}$$

Equation 4

Where,
T_o – operative temperature (°C)
T_{air} – air temperature (°C)
MRT – mean radiant temperature (°C)

Equation 4 is a simplified method of calculating T_o and is only relevant for occupants who are not exposed to direct sunlight or to air velocities greater than 0.20 m/s. (ANSI/ASHRAE Standard 55, 2010)

3.1.2.4 Adjusted mean radiant temperature (MRT_{Adj})

Direct solar radiation falling on a human body and its influence on comfort constitutes a significant part of this thesis, for which so-called solar adjusted mean radiant temperature (MRT_{Adj}) is considered a determining factor for thermal comfort calculations. MRT_{Adj}, as illustrated in *Figure 5*, represents an existing mean radiant temperature adjusted for shortwave solar radiation on a human body.

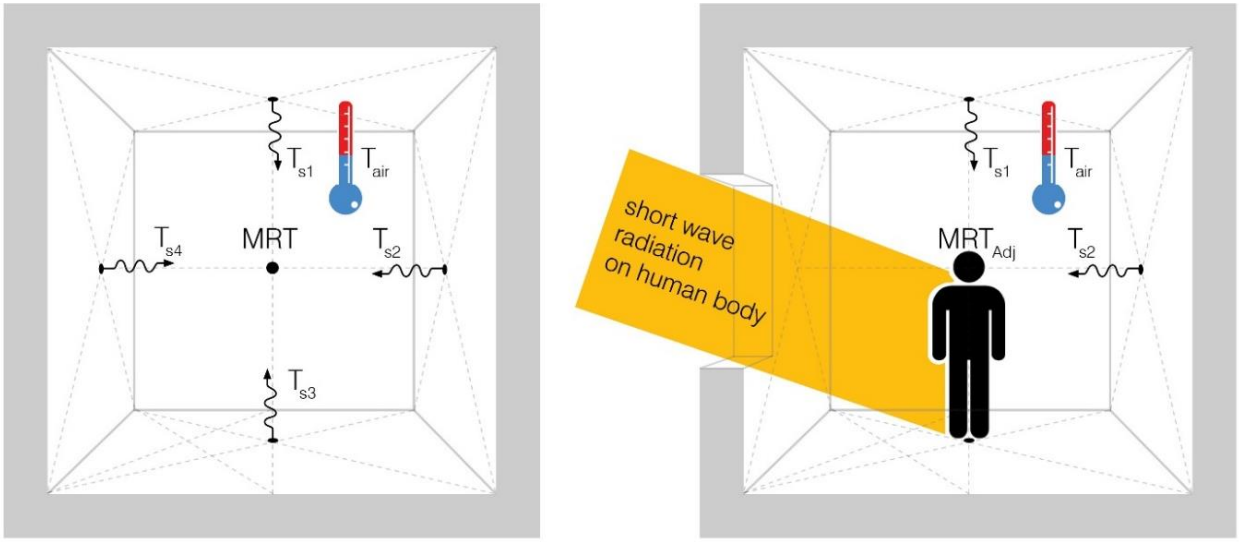

Figure 5: Temperature parameters of thermal comfort in a room without a window and a room with a window, where T_s - surface temperature, MRT - mean radiant temperature, MRT_{Adj} - solar adjusted MRT, T_{air} – air temperature.

The short wave radiation falling on an occupant is translated into an effective radiant field and solar adjusted mean radiant temperature according to SolarCal method. (Arens & Hoyt & Zhou, 2015)

SolarCal method

The SolarCal model is based on the effective radiant field, *ERF*. *ERF* is a measure of additional radiant heat flux to or from the human body and it can be calculated for an occupant exposed to both long-wave exchange with surfaces and short-wave radiation.

The surrounding surface temperatures are represented as *MRT*, which can be related to *ERF* (from long-wave exchange with surfaces) according to *Equation 5:*

$$ERF = f_{eff} * h_r * (MRT - T_{air}) \qquad \textit{Equation 5}$$

Where,
f_{eff} - fraction of the body surface exposed to radiation from the environment (0.696 for a seated person)
h_r - radiation heat transfer coefficient (W/m^2 K)
T_{air} - air temperature (^{o}C)

When short-wave radiation absorbed on the body's surface is considered, the additional solar radiation flux, ERF_{solar}, can be calculated according to *Equation 6:*

$$ERF_{solar} = (0.5 * f_{eff} * f_{svv} * (I_{diff} + I_{TH} * R_{floor}) + (A_p * f_{bes} * I_{dir}/A_D) * T_{sol} (\alpha_{SW}/\alpha_{LW}) \qquad \textit{Equation 6}$$

Where,
f_{svv} - fraction of sky vault in occupant's view
I_{diff} - diffuse sky irradiance received on an upward-facing horizontal surface (W/m2)
I_{TH} - total outdoor solar radiation on the horizontal plane (W/m2)
R_{floor} - reflectance of the floor
A_p - projected area of the body
f_{bes} - fraction of body exposed to sun
I_{dir} – direct beam (normal) solar radiation (W/m2)
A_D - the DuBois surface area of the assumed person (ca. 1.8 m2)
T_{sol} – total solar transmittance of a window system
α_{SW} - short-wave absorptivity (0.67 for white skin and average clothing)
α_{LW} - long-wave emissivity/absorptivity, typically equal to 0.95

Hereafter, MRT_{Adj} can be calculated by adding ERF_{solar} to the longwave *ERF*, and proceeding according to *Equation 5.*

3.1.2.5 Adjusted operative temperature ($T_{op,\ Ajd}$)

Solar adjusted operative temperature $T_{op,Ajd,}$ is obtained using Equation 7*:*

$$T_{op,Adj} = \frac{T_{air} + MRT_{Adj}}{2} \qquad \textit{Equation 7}$$

Where,
$T_{op,Adj}$ – solar adjusted operative temperature (°C)
T_{air} – air temperature (°C)
MRT_{Adj} – solar adjusted mean radiant temperature (°C)

3.1.3 Comfort models

Currently, two models aiming to quantify perceived thermal comfort coexist. One model, Predicted Mean Vote (PMV) is based on the static heat balance of the body and the second model, adaptive model, considers the human thermoregulatory system's ability to adapt to its surroundings. (Brager & de Dear, 2001)

3.1.3.1 Adaptive comfort

"The adaptive model, which states that factors beyond fundamental physics and physiology play an important role in impacting people's expectations and thermal preferences" (Brager & de Dear, 2001).
The adaptive model is based on research done on field studies. The model refers to the human mechanisms of acclimatization being paramount to the way in which comfort is individually perceived. (Brager & de Dear, 2001).

3.1.3.2 Swedish recommendations

The Swedish department of health recommends operative temperature not to exceed 26°C for an extended period of time. (Folkhälsomyndigheten, 2014)

3.2 Ray tracing

Ray tracing is a method for tracking light rays coming into a space and is as a result a method of rendering three-dimensional graphics with very complex light interactions. There are various types of ray tracing including backward, forward and hybrid ray tracing. For the purposes of this thesis, backward ray tracing is used, which implies that eyes are the light source and hereby source of the rays. The rays are further called solar vectors. The main principle or backward ray tracing and solar vectors bouncing off surfaces is shown in *Figure 6*. (Radiance, 2015).

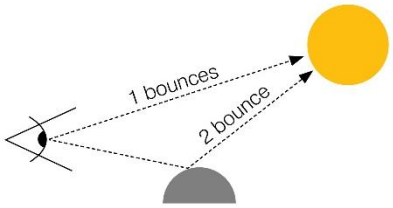

Figure 6: Backward ray tracing with 1 and 2 bounces.

3.3 View factor

View factor is a geometric quantity between 0 and 1 and describes the exchange of energy between two surfaces. Radiation heat exchange between surfaces depends on the orientation of the surfaces relative to each other. This dependence on orientation is accounted for by the view factor. (Cengel Y. A., 2011). As seen in *Figure 7*, the orientation of a surface highly impacts the radiative heat exchange to which the point is exposed.

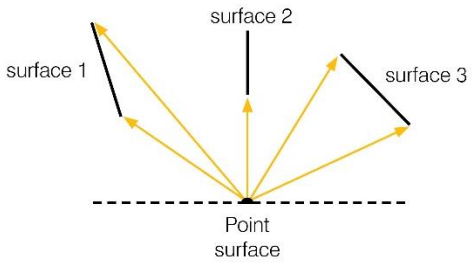

Figure 7: View factor concept.

4 Method

4.1 Overview / Project structure

The structure of the project comprises four steps, illustrated in *Figure 8.* The initial step, Step 0 is where the building geometry is modelled in Rhino. The following three steps constitute the core of the shade-tracing method/tool developed in this thesis.

Step 1 is the thermal module, which analyses how thermal comfort is affected by solar gains in the existing geometry. Step 2 comprises the data module, handling and processing thermal results in Excel and Step 3, is the ray tracing module, which interprets shading need based on comfort results and redistributes *g*-value accordingly.

For iterative purposes, Step 4 was introduced. Step 4 follows the same methodology as Step 1, analyzing the effect of redistributed *g*-value on thermal comfort, enabling validation of the tool.

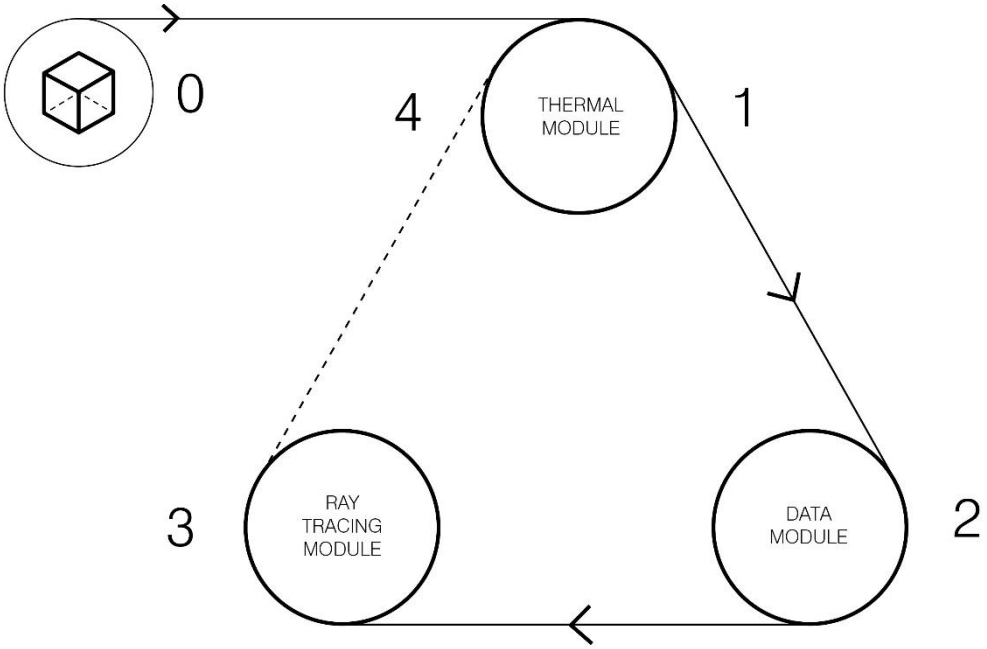

Figure 8: Project structure.

Step 1-3, has a defined input/output flow of information. Input to one step can be either output from the previous step or input of external data. All information outputted by one module and continuing to the next module, indicated by the arrows in *Figure 8*, is considered to be intermediate output, essential for the functionality of the tool but not extracted as results. Details of the input/output and intermediate output are explained further in the Method section.

4.2 Software

The software tools utilized in the scripting of the tool were chosen due to their interoperability, alleviating the flow from tedious importing and exporting format collisions.

Each step explained in *Figure 8* has corresponding tools, depicted in *Figure 9*. It should be noted that, the operability of the used scripting tool Grasshopper, and consequently the environmental plugins Ladybug and Honeybee, rely on the geometry being modelled in the modelling tool Rhinoceros, for which Rhino was integrated in all the steps of the tool, but for illustrative reasons, is only included once in *Figure 9.*

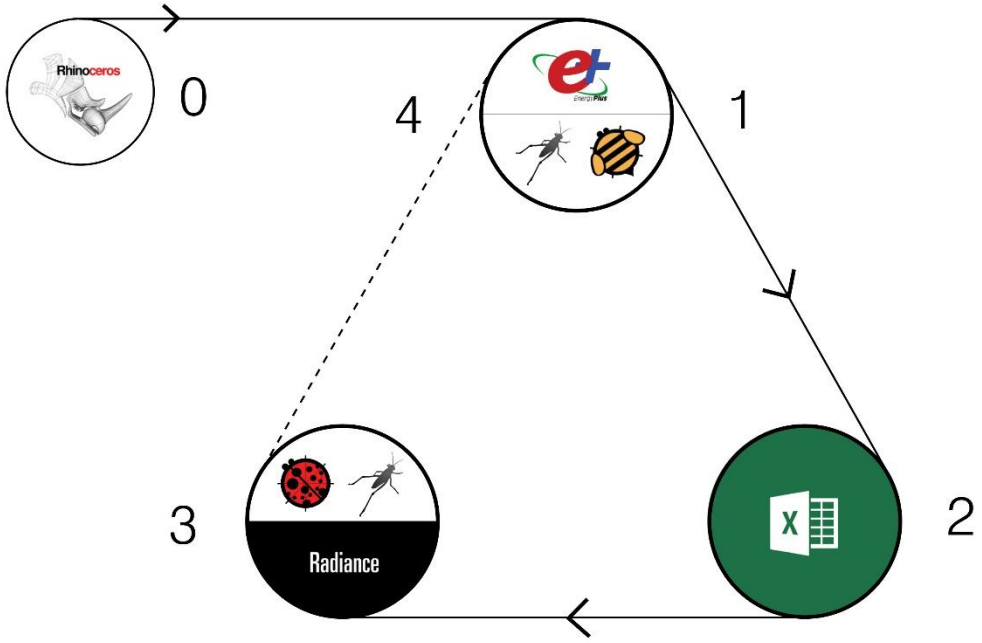

Figure 9: Software used in each step of the method.

4.2.1 STEP 0

Rhinoceros

Rhinoceros (shortened Rhino) is a commercial three-dimensional computer-aided design software, based on NURBS mathematical model, which is used for modelling a wide variety of products, including architecture modelling (McNeel, 2015). Rhino uses Boundary Representation (Brep) to compose 3D objects and be able to perform geometry manipulations (McNeel, 2015).

4.2.2 STEP 1/ STEP 4

Energy Plus

EnergyPlus is a whole building energy simulation program that engineers, architects, and researchers use to model both energy use — for heating, cooling, ventilation, lighting, and plug and process loads—and water use in buildings. (EnergyPlus, 2015)

Grasshopper

The Grasshopper (*GH*) plu*g*-in is a graphical algorithm editor integrated within Rhino 3D CAD environment. The program allows a dynamic interaction with 3D geometry within Rhino, where all geometric changes are virtual, using the Rhino viewport to display the results of the GH definition. (grasshopper3d, 2015).

Terminology used in the report to describe work done in grasshopper:

- Component – a building-block that performs a specific action
- Definition – a network of grasshopper components - your Grasshopper 'model'
- Parameter – a special component that contains data (values) instead of performing an action

Honeybee

Honeybee (*HB*) is an open source environmental plugin for Grasshopper, enabling interaction with simulation engines of EnergyPlus, Radiance, Daysim and OpenStudio for building energy and daylighting simulations (grasshopper3d, 2015).

4.2.3 STEP 2

Excel

Excel is a computer program which name stands for Electronic Spreadsheet Program. Storing, organizing and manipulating data are the main functions of Excel.

4.2.4 STEP 3

Radiance

Radiance is a lighting simulation tool making use of ray tracing methods i.e. backward ray tracing. (Radiance, 2015). Radiance is the base upon which Ladybug and Honeybee perform ray tracing analysis (for solar gains and daylight).

Ladybug

Ladybug is an open source environmental plugin for Grasshopper. With the aim to help architects and engineers create an environmentally-conscious building design, Ladybug imports standard EnergyPlus Weather files (.EPW) into Grasshopper (grasshopper3d, 2015).

4.3 Shade-tracing tool

4.3.1 STEP 0: Building geometry

A freestanding “shoebox” building with one thermal zone was modelled in Rhino, see *Figure 10.* No furniture or interior details were considered. This building geometry was used throughout the method.

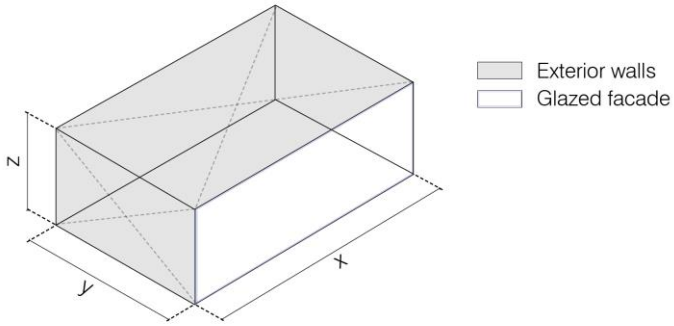

Figure 10: Geometric model on which analysis was made.

4.3.2 STEP 1: Thermal module

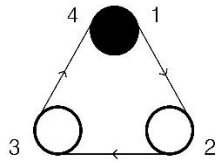

The geometry introduced in Step 0 was thermally modelled in Honeybee (*HB*) and simulated with EnergyPlus engine in *HB*. The climate file, necessary model inputs and analysis period(s) and point(s) were defined and the intermediate thermal output attained was hereafter exported to Excel. All stages of the modelling were established as definitions in Grasshopper (*GH*).

Climate file

A valid .epw file and .stat file were inputted.

Geometric model input

The following model input, specific for the analyzed building case, were defined:

- Construction
  - Construction type for each surface i.e. façade, roof, floor and internal walls.
  - Thermal properties for each construction type including *U*-value.
  - If context or shading geometry were present in the model, the construction was considered to be opaque. No other material properties for context were considered.
- Glazing
  - Material properties of glazed surface
    - *g*-value
    - *U*-value and
    - Visible transmittance (VT)

Envelope surfaces encompass the thermal zone in which all simulations were carried out. The zone loads and schedules assigned were as follows:

- Loads and schedules
  - Zone loads and schedules for including equipment, lighting, infiltration, occupancy, ventilation per area and per person.

Analysis period

The period for which the thermal simulation was run was defined as an annual per default. All hours which were not occupied during the analysis period were removed from the output, in order to only account for overheating hours which were occupied.

Analysis point(s)

In order to simplify output and shorten output, thermal comfort parameters were analyzed for one point only. The point coordinate (x; y; z) were selected by dividing the floor surface into a desired grid. The center-points of the floor grid are the resulting sensor points for the study.

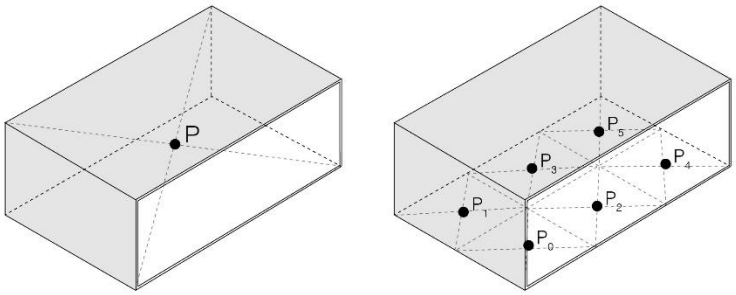

Figure 11: Location of sensor point in EnergyPlus thermal simulations, Point P and the mapped sensor Points 0, 1, 2, 3, 4, 5

Simulation results

The thermal results from the EnergyPlus engine consisted of temperature parameters for the analyzed zone during the analysis period. These results were post-processed in order to achieve results for a chosen analysis point and further adjusted to include the influence of direct solar radiation.

The post processing was performed utilizing an existing *HB* component based on the SolarCal method, described in *Section 2.1.3.5 Adjusted MRT*. The component, *"Microclimate map"* (Mackey, 2015), enables mapping of initial EnergyPlus comfort results according to a chosen grid size, comfort model. The component required input about an analysis point's view factor and four thermal outputs from EnergyPlus simulation results, namely, average air temperature, air heat gain (for air stratification calculation), incoming airflow (also for air stratification) and indoor surface temperatures.

Moreover, the *Microclimate map* component incorporates the effect of direct solar radiation to the comfort analysis, enabling results of adjusted thermal parameters of $T_{op,Adj}$, MRT_{Adj} *and* T_{air} for the chosen analysis period and point(s) to be retrieved and exported to excel in Step 2 for further handling. Hereby the comfort temperature parameters are considered to be an intermediate output, as explained in *Section 3.1 Overview.*

4.3.3 STEP 2: Data module

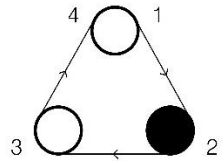

The steps taken to interpret thermal modelling output from Step 1 in Excel are presented below. The external input required in Step 2 was the adjusted operative temperature threshold above which point(s) experiencing overheating were further analyzed in Step 3. The intermediate output of Step 2, used as input for Step 3, is the solar overheating factor, explained further below. The result of Step 2 is graphical interpretations including duration diagrams and time distribution of overheating data.

$T_{op,Adj}$ threshold input

A single operative temperature threshold was required, in order to remove hourly data which was not considered uncomfortable and limit the raw data handling in Excel e.g. 26°C.

Local shading need evaluation

To evaluate shading need for point(s) exposed to direct solar radiation, a relation between thermal discomfort and shading need had to be determined.

Since air temperature is independent of solar radiation, the solar influence on operative temperature was derived from the difference between MRT and operative temperature. This, based on the simplified temperature relationship specified in *Equation 8*.

$$\Delta T = MRT_{Adj} - T_{op,Adj} \qquad \textit{Equation 8}$$

Where,
ΔT – derived impact of solar radiation on solar adjusted operative temperature
MRT_{Adj} – solar-adjusted mean radiant temperature (°C)
$T_{op,Adj}$ – solar-adjusted operative temperature (°C)

Hereby, a larger ΔT implies a larger impact of solar radiation on adjusted operative temperatures at a certain point, and a greater shading need can thus be expected. A negative ΔT implies that a point experiences no solar contribution. Hours experiencing negative ΔT were ignored in further calculation.

Solar overheating factor, ΔT *factor*

To implement the influence of ΔT on shading need, a solar overheating factor, ΔT *factor*, was introduced. The factor is between 0 and 1, where a factor of 1 is allocated to points experiencing the largest contribution of solar gains on thermal discomfort, ΔT_{max} during the analysis period.

Remaining ΔT values are linearly scaled according to ΔT_{max}. When $MRT_{Adj} = T_{op,Adj}$,, there is no relative solar contribution on experienced discomfort, for which a factor of 0 is allocated. See *Figure 12*.

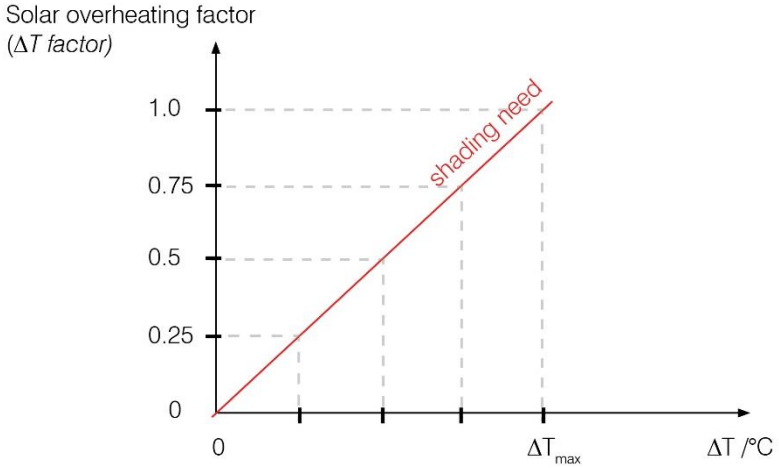

Figure 12: Shading need of an intersection point as a linear relation between ΔT and solar overheating factor.

As output, an excel spreadsheet with calculated ΔT *factors* for every hour of analyzed period and coordinates of the sensors, is generated, as shown in *Table 1*.

Table 1: Example of excel spreadsheet with ΔT factors for analysis points (column A) and hours of analyzed period (row 1), where x,y,z represents coordinates of each point.

1	Hour of the year	3802	3803	3804	3805	3806	3807	3808	3809	3810
2	x_0, y_0, z_0	0.00	0.32	0.31	0.41	0.26	0.23	0.20	0.00	0.00
3	x_1, y_1, z_1	0.00	0.23	0.23	0.24	0.21	0.19	0.17	0.00	0.00
4	x_2, y_2, z_2	0.00	0.37	0.56	0.51	0.49	0.29	0.25	0.00	0.00
5	x_3, y_3, z_3	0.00	0.23	0.23	0.24	0.21	0.19	0.17	0.00	0.00
6	x_4, y_4, z_4	0.00	0.59	0.59	0.53	0.52	0.30	0.26	0.00	0.00
7	x_5, y_5, z_5	0.00	0.25	0.25	0.26	0.23	0.20	0.18	0.00	0.00

4.3.3.1 Thermal data output

Duration diagrams

Graphs showing the duration for which $T_{op,Adj}$ exceeds assigned threshold temperature for the analysis point during the analysis period.

Time distribution

Hourly and weekly time distribution was analyzed to show which hours of the day the analysis points were receiving the highest temperatures. This was done with Grasshopper native components. The time distribution was further combined with cloud cover from the weather data file to give a better understanding of the output.

4.3.4 STEP 3: Ray tracing module

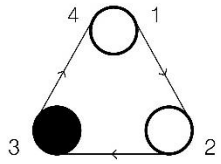

The ray tracing module includes four stages of processing data: ray tracing intersection points, calculating shading area, re-distributing *g*-values and rearranging frit pattern on the façade. All four stages of the processing were established as definitions in Grasshopper (*GH*).

4.3.4.1 Ray tracing definition

Ray tracing definition was created for locating and visualizing intersection points on the façade. The definition was based on backward ray tracing method see *Section 3.2 Ray tracing*, utilizing the Ladybug component *"Bounce_From_Surface"* in GH. The component generates the solar vectors directed from the sensor points to the sun. The number of bounces was set to 1 and the direct solar vectors were traced.

Solar vectors were traced for hours of the year when solar radiation contributes positively to discomfort (ΔT *factors* > 0), for which the intersection points between the vectors and the glazing were established and recorded in *GH*.

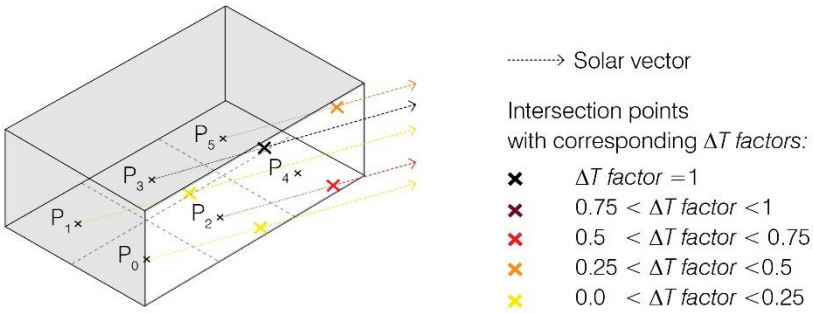

Figure 13: Solar vectors, generated with backward ray tracing. Intersections with the glazed façade are illustrated by the crosses.

4.3.4.1.1 Ray tracing output

The ray tracing definition outputs the pattern of intersections of solar rays on the façade for a desired analysis period. The pattern represents the position and ΔT *factors* of intersection points, as shown graphically in *Figure 14*. The colors represents a threshold of ΔT *factor*, illustrating the relative impact of overheating from each intersection. The ΔT *factor* is described in *Section 4.3.3 STEP 2: Data Module*. The output was further handled for calculating areas of shading frit and *g*-values of glazing units as described in *Section 4.3.4.2 Shading area definition* and *Section 4.3.4.3 Redistributed g-value definition*, accordingly.

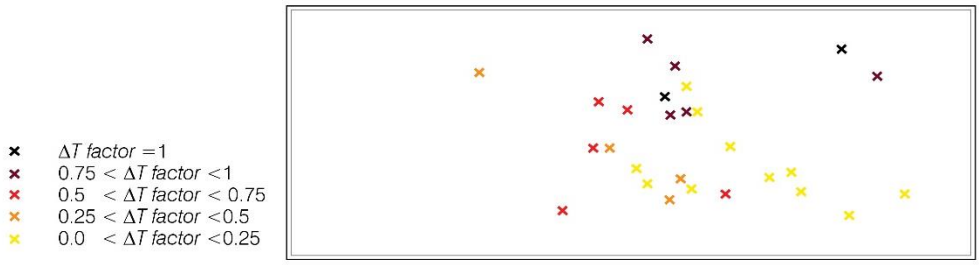

Figure 14: Position of the intersection points with equivalent thresholds of ΔT factors on the façade.

4.3.4.2 Shading area definition

A shading area definition was created to determine the shading frit size, according to its position on the façade. By adopting *Equation 3*, frit was applied to the facade to reduce the average *g*-value.

The calculation of shading area requires input of average *g*-value of a glazed façade (g_{ave}), non-shaded glass *g*-value and frit transparency (TR_{sh}). Moreover, the following two conditions must be met:

1. Non-shaded glass *g*-value need to be higher than desired average *g*-value
2. Frit transparency need to be lower than the desired average *g*-value

The total area of shading frit needed is calculated according to *Equation 9*:

$$A_{sh} = \frac{g_{ave} - g_{non-shaded}}{TR_{sh} - g_{non-shaded}} \times A_{facade}$$ *Equation 9*

Where,
g_{ave} – average *g*-value of the facade
A_{sh} – Total shading frit area need, m^2
A_{facade} – Total façade area, m^2
TR_{sh} – Shading frit transparency
$g_{non-shaded}$ – Non-shaded glass *g*-value

The main principle of the area need calculation is illustrated in *Figure 15.*

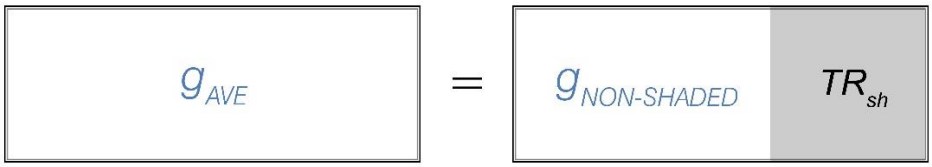

*Figure 15: Facade g-*value *calculation principle.*

The single frit area corresponding to the shading need (Δ*T factor)* at each intersection point on the façade, is calculated as follows:

$$A_{\Delta Tfactor} = \frac{A_{sh}}{\sum_{\Delta Tfactor}}$$ *Equation 10*

Where,
$A_{\Delta Tfactor}$ – Single frit area relative to Δ*T factor*, m^2
$\sum_{\Delta Tfactor}$ – Sum of all Δ*T factors* at intersection points on the facade
A_{sh} - Total shading frit area need, m^2

The main principle of a single frit relative area calculation is illustrated in *Figure 16.*

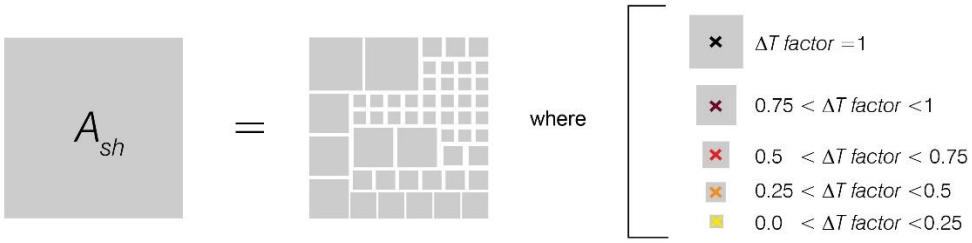

Figure 16: Single frit relative area calculated according to corresponding Δ*T factor.*

4.3.4.2.1 Shading area output

The shading area definition outputs a non-uniformly distributed frit pattern, as shown in *Figure 17*. Each geometry of frit was assigned to location of the corresponding intersection points (see *Section 4.3.4.1 Ray tracing definition*).

As illustrated in *Figure 17*, resulted frit surfaces are likely to overlap, which reduces the absolute area of the shading. In order to obtain a frit pattern, which meets the need of the total shading frit area, each frit was scaled according to the previously assigned Δ*T factor*.

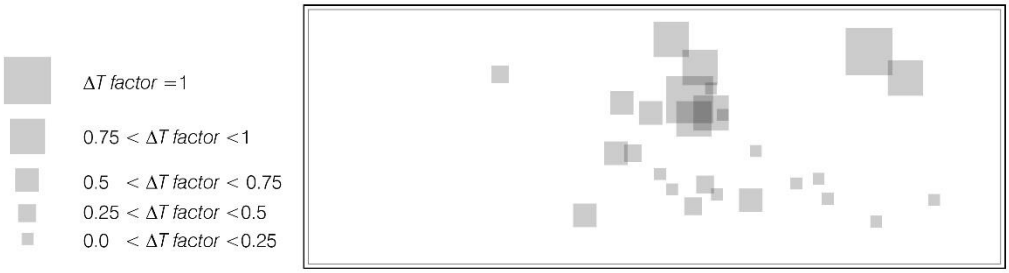

Figure 17: Resulted non-uniformly distributed frit pattern.

4.3.4.3 Redistributed *g*-value definition

Large glazed areas, such as glazed facades, are commonly divided into grids of smaller glazing units, see *Figure 18.* As described in *Section 3.1.1.3.2 Shading coefficient of fritted glass* a glazing unit may have a specific *g*-value.

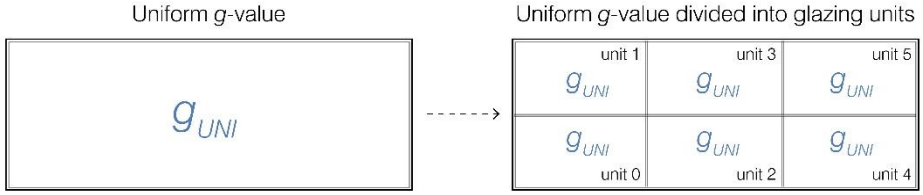

Figure 18: Facade with uniform g-value of glazing before and after being divided into a grid of six glazing units.

Re-distributed *g*-value definition was created in order to distribute *g*-values on the glazing units of the façade corresponding to the need for shading indoors, determined according to method described in *3.2 Ray tracing*. The shading area needed was determined according to method described in *Section 4.3.4.2 Shading area definition.*

A shading area needed was calculated for every glazing unit according to *Equation 11.* The higher the sum of ΔT *factors* within a glazing unit, the higher the shading area needed for that glazing unit.

$$A_{sh,unit} = \sum_{\Delta T factor,unit} \times A_{\Delta T factor} \qquad \textit{Equation 11}$$

Where,
$A_{sh,unit}$ – Shading area needed for a glazing unit, m^2
$A_{\Delta T factor}$ – Single frit area relative to ΔT *factor,* m^2
$\sum_{\Delta T factor,unit}$ - Sum of ΔT *factors* within a glazing unit

After the shading area need for each glazing unit was defined, the g-value for each glazing units *(g_{unit})* could be calculated according to *Equation 12*. It was assumed that the average *g*-value of a glazing Shading coefficient of fritted glass. Hereby, resulting glazing unit g-value is highly dependent on previously calculated shading frit area need, transparency of shading and non-shaded glass g-value.

$$g_{unit} = \frac{(A_{sh} * TR_{sh}) + ((A_{unit} - A_{sh}) * g_{non-shaded})}{A_{unit}} \qquad \textit{Equation 12}$$

Where,
A_{unit} – Area of a glazed unit, m^2
A_{sh} – Total shading area need, m^2
TR_{sh} – Frit transparency
$g_{non-shaded}$ – Non-shaded glass *g*-value

4.3.4.3.1 Redistributed *g*-value output

The redistributed *g*-value output included a list of *g*-values between 0 and 1. The number of *g*-values correspond to the number of glazing units which the façade was divided into.

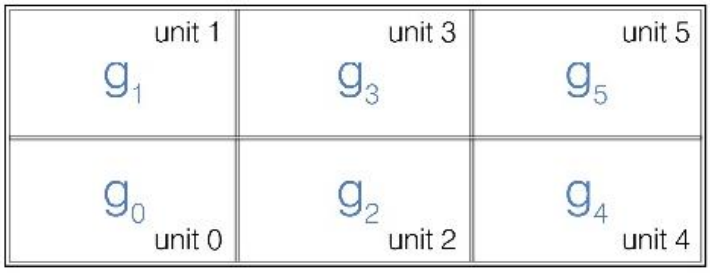

Figure 19: Glazed facade divided into 6 glazing units, with corresponding g-values assigned to each unit

Resulting *g*-values below zero suggest that the shading need was greater than what is achievable by reducing the *g*-value. Hereby, if resulted *g*-value were negative, the non-fritted glass *g*-value needed to be lowered to compensate for the higher shading need.

4.3.4.4 Uniformly distributed frit pattern

Alternatively to the redistributed *g*-value, a geometry of uniformly distributed frit pattern could be generated. The calculation was performed based on a single frit area (A_{frit}). The number of single frits (F) per glazing unit was individually calculated according to *Equation 13.*

$$F = \frac{A_{frit,unit}}{A_{frit}} \qquad \textit{Equation 13}$$

Where,
F - Number of frits per glazing unit
A_{frit} - Area of a single frit, m^2
$A_{frit,unit}$ – Total frit area needed for a glazing unit, m^2

The resulted number of frits were evenly distributed on a grid on the glazing unit.

4.3.4.4.1 Uniformly distributed frit pattern output

The redistributed *g*-value definition outputs either the values of calculated *g*-values or the uniformly distributed frit pattern by displaying them on the 3D model, as shown in *Figure 20.*

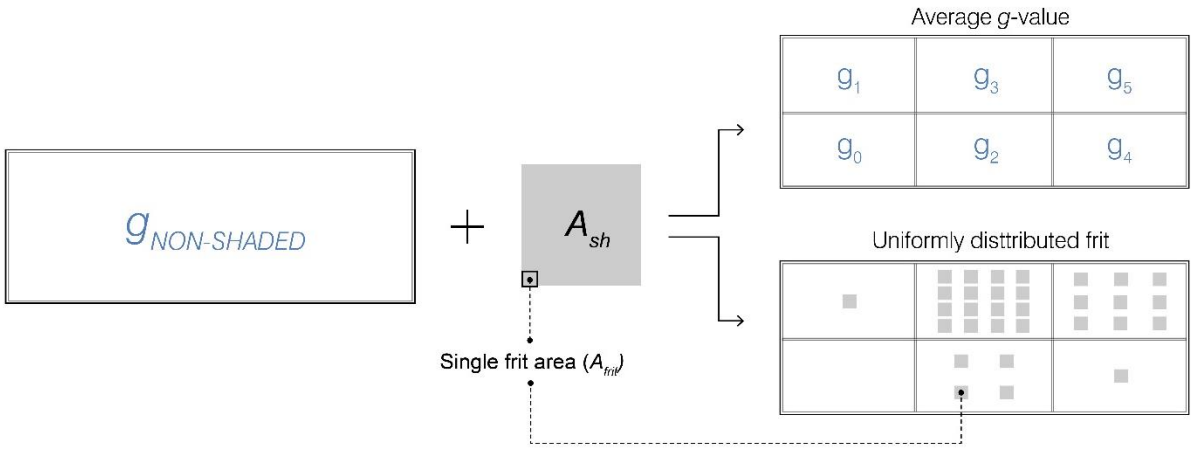

Figure 20: Glazed facade before and after distribution of g-values, Non-uniformly and uniformly distributed frit patterns.

4.3.5 STEP 4: Thermal iteration

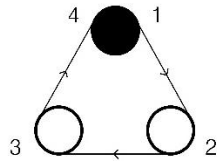

Step 4 represents an iterative step in the method, following the same procedure as in Step 1, aiming to test the solution provided in the ray tracing module in Step 3. Step 4 aimed to confirm the functionality of Step 0-3 of the tool.

In Step 4, there is an exception to the methodology explained in Step 1 and that is how the glazed façade(s) is modelled in Honeybee. The glazed surface(s) were divided into units, or sub-surfaces, representing size of glazing used in the Step 3, see *Figure 21*. The resulting redistributed *g*-values, referred to as average *g*-values from Step 3 were assigned and the EnergyPlus simulation was rerun.

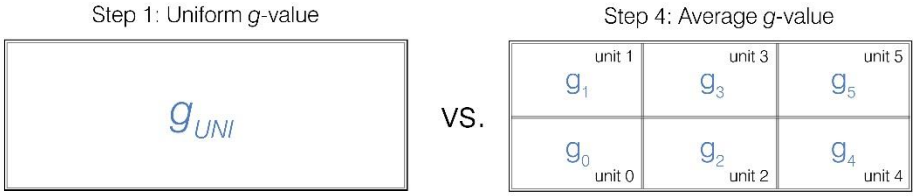

Figure 21: Glazed facade with corresponding g-values in Step 1 and Step 4, accordingly.

The results were exported and compared to the results from Step 2, results displayed in *Section 6 Results*.

4.4 Validation

4.4.1 Reference Case

The method and shade-tracing tool were tested on a Reference Case building. The settings used for the Reference case, following the project structure in *Section 4.1*, are illustrated in *Figure 22*.

STEP 0: Geometry

A simple "shoe box" geometry with dimension of 8 m·5 m·3 m was modelled in Rhino.

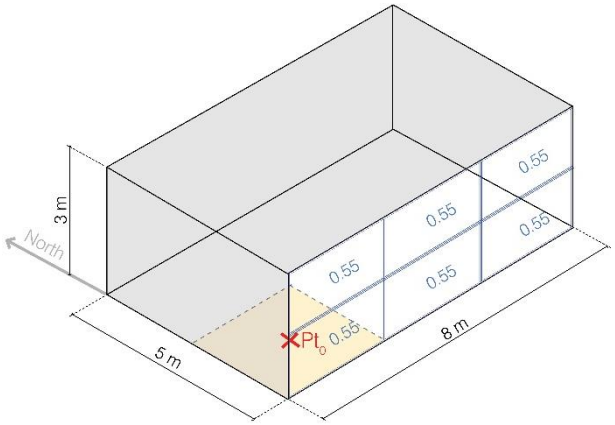

Figure 22: Reference Case geometry.

STEP 1: Thermal module

The floor of the geometry was divided into a grid of 3·2 divisions, with a one floor grid corresponding to an area of 2.7 m·2.5 m. One test point in, Point 0, was chosen to be analyzed in terms of thermal discomfort and shading need. The weather data used for the reference was Copenhagen climate file. The zone was set to be an office occupied on weekdays between 8 and 18, with a lunchbreak between 12 and 13. The density of people was 0.05 people/m^2 (Blomsterberg & Dalman & Gräslund & Henriksson & Jansson & Jonsson & Kellner & Levin & Sjögren, 2013).

Annual thermal simulations were made, measuring the impact on adjusted operative temperature before and after applying the method/tool.

Glazing type and grid

The southern façade was fully glazed, resulting in a glazing to floor ratio (*GFR*) of 60%. In EnergyPlus. All glazing, was modelled with Simple window indices explained *in Section 3.1.1.2.1 Simple window indices.* The following double glazing type was used for the Reference case throughout the study.

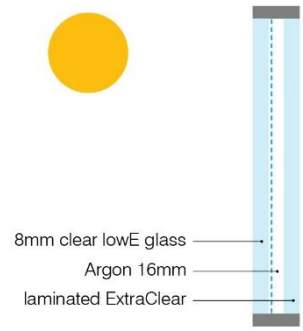

Figure 23: Reference glazing unit.

Table 2: Reference glazing unit physical properties.

Glazing	*LT* / %	*g*-value	*U*-value / W/(m^2·K)
Double glazing unit (*DGU*) Outer pane: 1. 8 mm clear Low-E glass Cavity: 2. 16 mm argon Inner pane: 3. 44.2 mm laminated float glass	78	0.55	1.1 (vertical) 1.7 (inclined)

Construction

Materials from the EnergyPlus material library were assumed, with *U*-values as close to recommended values (Blomsterberg & Dalman & Gräslund & Henriksson & Jansson & Jonsson & Kellner & Levin & Sjögren, 2013). It is possible to personalize the constructions but for the purpose of simplifying the method, available constructions were utilized.

Table 3 Construction details for the Reference case

Construction element	*U*-value /W/(m^2·K)
Ground floor	0.56
Roof	0.16
Wall	0.22

Construction airtightness of 1.8 l/(s·m^2) at 50 Pa was chosen according to Swedish airtightness requirements for office buildings. (Blomsterberg, 2007)

Ventilation

The ventilation system employed to the Reference case is an ideal load system. The cooling/heating set point is the indoor temperature above/below which the cooling/heating system is turned on. The cooling/heating setback is the indoor temperature that the space will be kept at when it is unoccupied. (Roudsari, 2015) The temperature set points and setbacks are presented *Table 4.*

Table 4 Heating and cooling set point and set back temperatures for Reference Case

Cooling set point	24 °C
Cooling setback	26.7 °C
Heating set point	21 °C
Heating setback	15.6 °C

Heat gains

Heat gains of 7.6 W/m² and 9.0 W/m² were set for the Reference case, according to common heat gains in a modern office building in Sweden. (Blomsterberg, 2007)

Comfort model

An adaptive comfort model was assumed for the Reference Case, since it was considered to provide most realistic interpretation of thermal comfort considering the influence of solar adjusted comfort parameters.

STEP 2: Data module

According to national recommendations for indoor operative temperature, (Folkhälsomyndigheten, 2014), a thermal comfort threshold temperature of 26°C was chosen for adjusted operative temperature.

STEP 3: Ray tracing module

The optical properties of glazing are input to the shade-tracing tool, as follows:
Non-shaded glass *g*-value: 0.7
Average glass *g*-value 0.55
Shading frit transparency: 0.0

STEP 4: Thermal iteration

The fully glazed southern façade was divided into 6 modules with dimensions of 2.7 m·1.5 m, and the *g*-value was distributed according to solutions attained in Step 3.

4.4.2 Sensitivity study

The tool was evaluated by performing sensitivity studies on various parameters. Results were compared with regards to time distribution of temperatures above a set comfort threshold before and after distributing the *g*-value according to the method presented in *Section 4.3 Shade-tracing tool*.

The parameters analyzed in the sensitivity study are described below:

4.4.2.1 Frit geometry

Instead of varying the *g*-value of the glazing unit, it was of interest to test the tools applicability to change the *g*-value of glazing by applying physical shading on the exterior of the glass. This was done by introducing frit shading to the simulations.

The following types of frit were tested:

- Uniformly distributed frit
- Non-uniformly distributed frit

The non-uniform frit pattern was scaled to compensate for area of overlapping frits.

4.4.2.2 Climate file

Two additional climates were chosen to assess the tool's sensitivity to exterior environmental conditions. 1. Madrid, Spain and 2. Abu Dhabi, United Arab Emirates. Madrid's temperate climate has hot summers and cool winters, is amongst Europe's highest receivers of sunshine. Abu Dhabi has a hot desert climate, with extremely hot summers and warm winters. The outcome of the tool for these climates were compared to the Reference Case simulations, performed with a Copenhagen climate file.

4.4.2.3 One point on the floor

In order to identify how the tool function for different locations in a space, thermal comfort for Point 1, Point 2, Point 3, Point 4 and Point 5 were analyzed and compared to the Reference case results (for Point 0). See *Figure 24* for layout of sensor points on the floor.

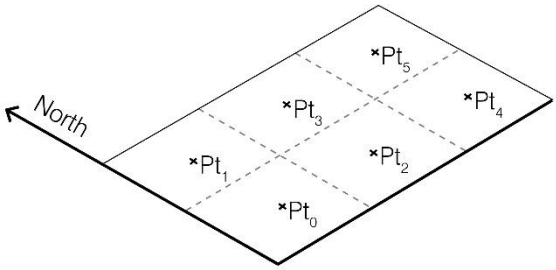

Figure 24: Location of sensors on the floor.

4.4.2.4 Several points on the floor

To evaluate the effect of the size of the analyzed area, three combinations of points were tested and compared to the Reference case results (for Point 0):

- Points 0 and 2
- Points 0, 1, 2, 3
- All points

4.4.2.5 Cooling set point temperature

Excess heat not blocked by shading devices or as a result of internal gains, can distort the effectiveness of the tool, since temperatures already amply exceeding comfortable levels cannot be removed by merely altering the *g*-value. Hereby, the ventilation set points may impact the outcome of the tool significantly, for which it was of interest to test the tool for different cooling set points. The following set point temperatures were analyzed and compared to the Reference case set point of 24 °C:

- No conditioning

- 28°C
- 26°C
- 22°C

4.4.2.6 Glazed facade grid

By minimizing the façade grid size, the problematic regions of the facade may become more defined, for which the outcome of varying the façade grid size is of interest.

The following divisions of the façade grid were tested and compared to the Reference Case division of 2·3:

- 2·2 (1.5 · 4.0 m)
- 3·4 (1.0 · 2.0 m)
- 5·6 (0.6 · 1.7 m)

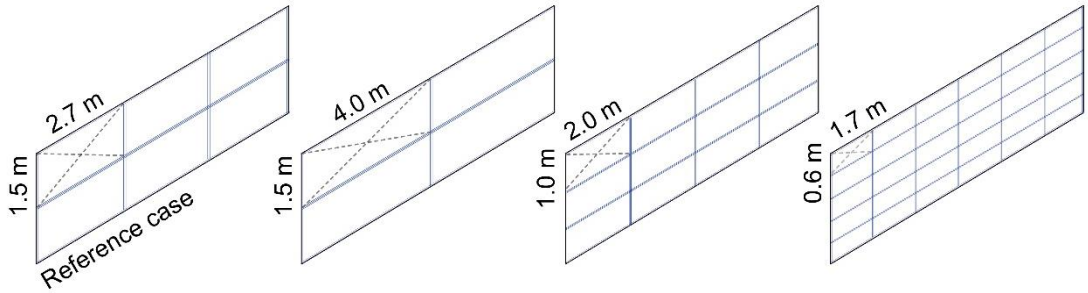

Figure 25: Divisions of the facade grid tested and compared to the Reference case (1.5x2.7 grid dimensions).

4.4.2.7 Factoring method

The factoring method used in the shade-tracing tool, described in *Section 4.3.3 Data module*, considers the effect of the direct solar component on thermal comfort and applies a ΔT factor between 0-1 accordingly. The ΔT factor used does not differentiate between any decimal values of the ΔT factor, for which the influence of smaller ΔT factors was of interest to analyze.

Firstly, the Reference case with ΔT factors between 0-1 was compared to a case with all ΔT factors >0 set to 1. The solar overheating factors for Point 0 were summed within every month and compared to the absolute sum of the solar overheating factors. Hereafter, the tool was tested on annual basis for four additional intervals of ΔT factors. All intervals are described in *Table 5*.

Table 5: Cases with different factoring methods tested in parametric study.

Case name:	Description:
1. Reference case	Case for which all positive ΔT factors were chosen
2. Factors 0.2-1	Case for which only ΔT factors with values higher than 0.2 were chosen
3. Factors 0.4-1	Case fir which only ΔT factors with values higher than 0.4 were chosen
4. Factors 0.6-1	Case for which only ΔT factors with values higher than 0.6 were chosen
5. Factors 0.8-1	Case for which only ΔT factors with values higher than 0.8 were chosen
6. Factors 1	Case for which all positive ΔT factors are replaced by values of 1 and as such used for g-value calculations

4.4.2.8 Orientation

The orientation of the glazed surface(s) play an important role as to when the space experiences solar gains. The influence of the building orientation was tested by rotating the building in an easterly and westerly cardinal direction and comparing the results to the Southerly orientation of the Reference case.

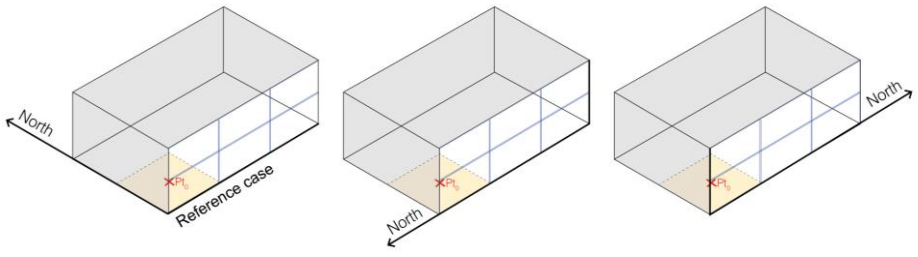

Figure 26: East and west-oriented facade tested.

4.4.2.9 Glazing ratio

The glazing ratio plays a significant role for the amount of direct solar heat gains entering a space. Similarly to the cooling set point temperature, the tool may be limited to the ratio of glazing. It is hereby of interest to analyze the method's functionality for spaces with varying glazing ratios.

The following glazing ratios were tested and compared to the Reference Case ratio of 60%:

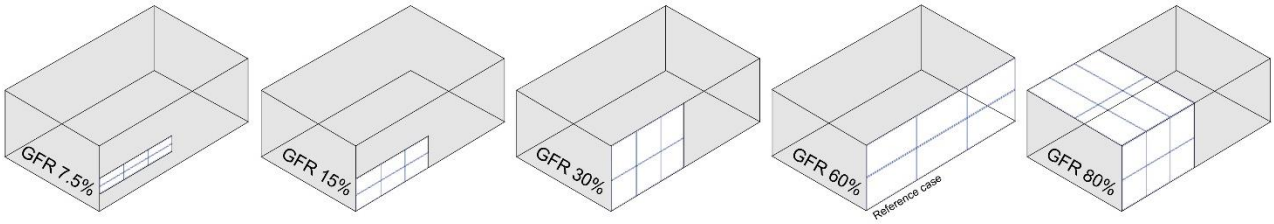

Figure 27: Four types of tested geometries with glazing to floor ratios of 7.5%, 15%, 30% and 80% in comparison to the Reference case with GWR of 60%.

For *GFR* 80%, the *U*-value of the horizontal glazing (roof) was increased to 1.7 W/m^{2}K to account for angular dependency of glazing *U*-value, see *Table 2.*

4.4.2.10 Average *g*-value of glass

By altering the average *g*-value of the facade, the thermal exchange upon which the method is based, is changed. Unexpected trends of altering this parameter could potentially limit the usability of the tool for cases with other thermal requirements of the envelope.

The distribution of the following initial *g*-value cases have been re-calculated and compared to the Reference Case average *g*-value of 0.55:

- 0.35
- 0.45
- 0.65

4.4.2.11 Analysis period

The period of time for which the tool is run, can influence how the output correlates to and affects the overheating problem. The analysis period was shortened and analyzed for:

- one season (summer),
- one month (August),
- one week (in August) and
- one day (2nd August)

Output for different analysis periods was compared to the Reference Case (with an annual analysis period).

4.4.2.12 Saving potential

Saving potential refers to the economic and environmental savings which could potentially be made by utilizing the tool for shading design. For example, economic savings could be made on glazing costs, by reducing the amount of solar controlled glazing used in a project. Furthermore, energy (and economic) savings could be made by reducing cooling loads. Additionally, solutions attained could hopefully increase daylight availability and views to the exterior, potentially improving the wellbeing of occupants.

The saving potential was investigated by increasing the average *g*-value of the façade until the temperature threshold of the sensor point surpassed a given limit.

5 Shade-tracing tool

5.1 Data flow

The resulting structure of the tool is shown in *Figure 28.* The model geometry is defined in Step 0 after which the following thermal modeling input is required for Step 1:

- grid size /density of the glazed façade
- *g*-value for initial uniform distribution of glazing
- buildings thermal input such as *U*-values of construction elements, heat gains and comfort model
- sensors on the floor for which thermal comfort was calculated
- occupancy schedule

The input data from Step 1 is processed in Honeybee and output to Excel as annual temperature data. In Step 2, a comfort threshold temperature needs to be defined. It is used to determine which data output from Step 1 is relevant further analysis. Two types of output are generated in Step 2:

- time distribution of overheated hours during a year
- solar overheating factors (ΔT *factors)* for every sensor and every hour of analyzed period

In Step 3, the module is supplied with: ΔT *factors,* the set points for shading transparency and non-shaded glass *g*-value. The following output can be achieved from Step 3:

- intersection points on the façade with corresponding ΔT *factors*
- new distribution of glazing with a range of *g*-values based on the calculated shading need
- frit pattern geometry

In Step 4, the effect of redistributed *g*-value on thermal comfort can be validated by iterating Step 1 to 3.

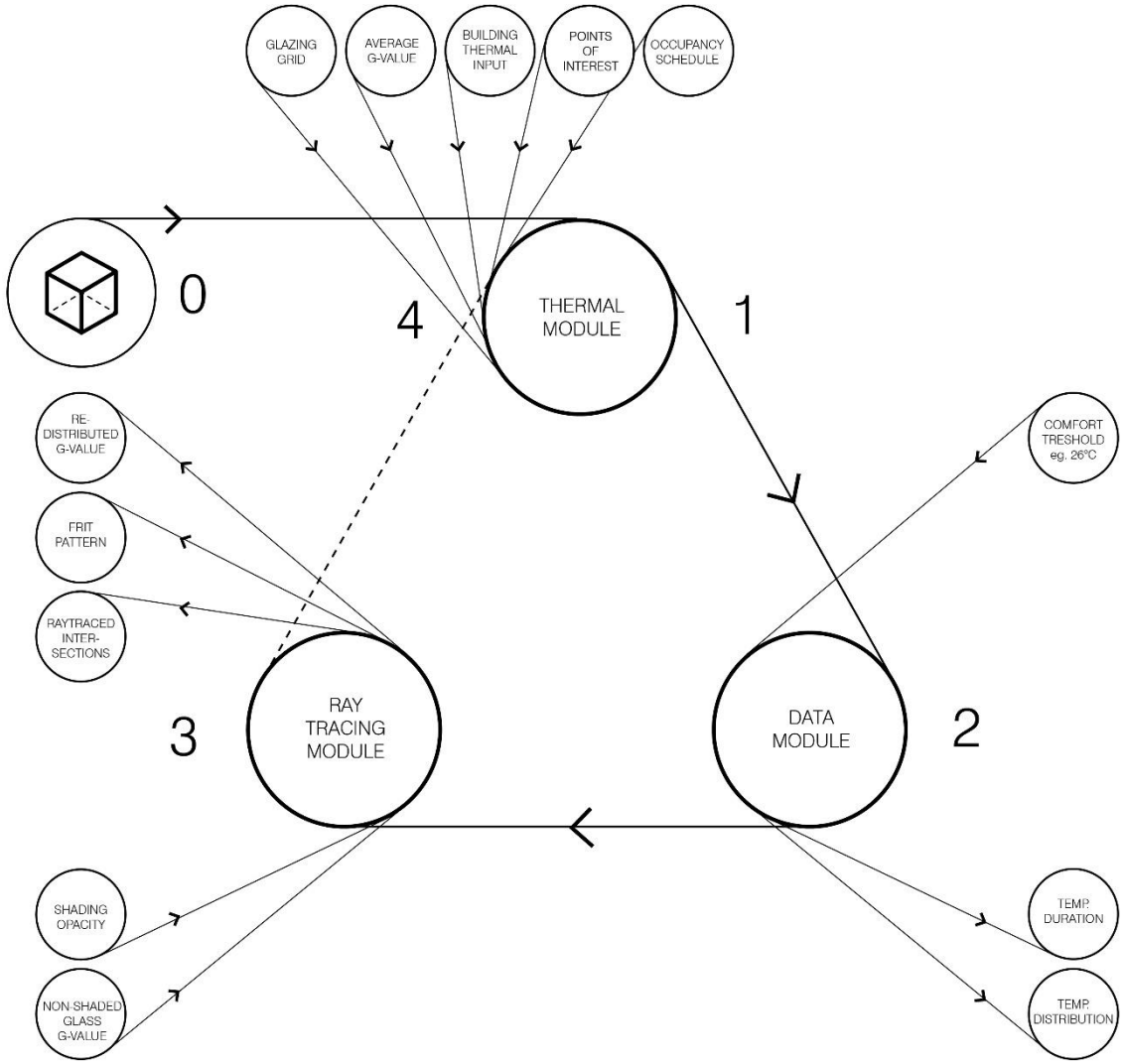

Figure 28: Resulted flow of input/output data through the tool.

6 Results

In this chapter, results are portrayed according to the principle shown in *Figure 29*. The uniform g-value represents a case before applying the method, while the average g-value stands for a corresponding case after application of the method.

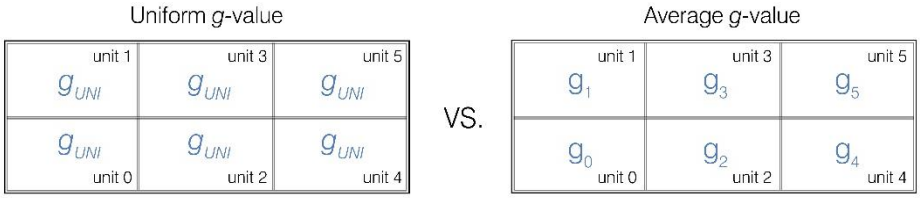

Figure 29: Glazed facade with uniform g-value and average g-value, for which results were obtained and are presented in the Section 6 Results.

6.1 Reference Case

Following the steps presented in the *Section 4.4.1 Reference Case*, results attained from the thermal module and ray tracing module were combined and compared to evaluate the tool.

6.1.1 Ray tracing module output

Ray traced intersections

The tool displays the distribution of intersection points on the façade with the corresponding values of solar overheating factors. The factors are categorized into five thresholds and colored-coded, see *Figure 30*.

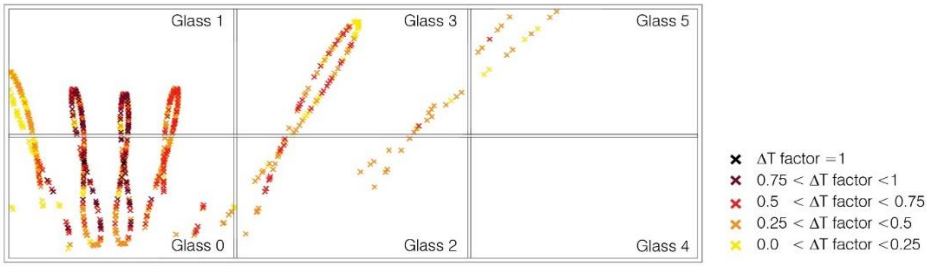

Figure 30: Distribution of intersection points with corresponding solar overheating factors in thresholds.

Re-distributed *g*-value

The tool redistributes *g*-value from a uniform distribution of 0.55 to an average distribution of 0.55 subsequently referred to as uni-g 0.55 and ave-g 0.55 respectively. This redistribution is displayed on the analyzed glazing as can be seen in *Figure 31*.

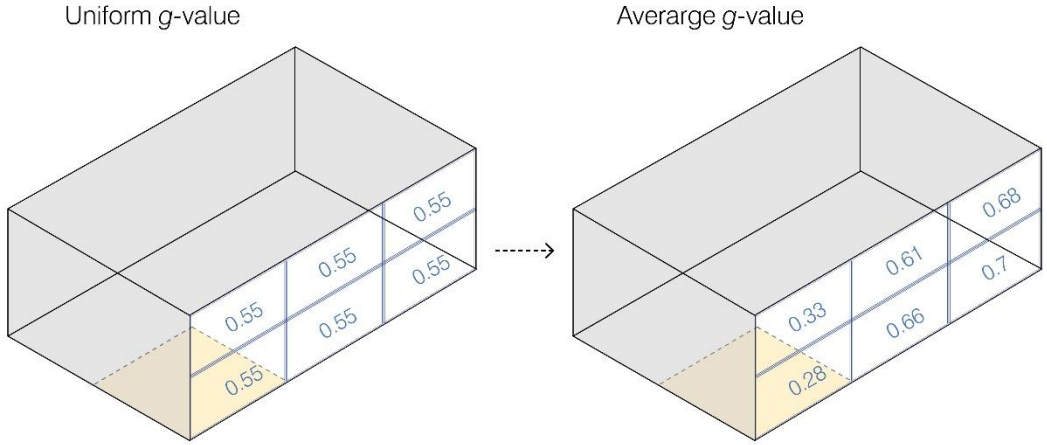

Figure 31: Distribution of g-values before and after applying the method.

Frit pattern

Following the problematic intersection points displayed in *Figure 30*, the tool presents two frit patterns, non-uniformly distributed frit (left), and translates this into uniformly distributed frit (right), see *Figure 32*.

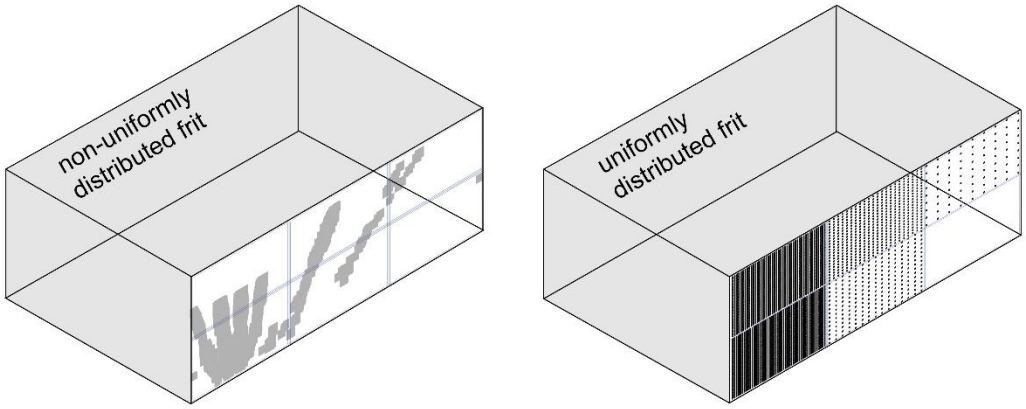

Figure 32: Graphic output of non-uniformly distributed frit and uniformly distributed frit patterns, respectively.

6.1.2 Validation output

Duration diagram - Adjusted operative temperature ($T_{o,Adj}$)

The distribution diagram was made on an annual basis for the Reference Case, for which the number of hours above a solar adjusted operative temperature ($T_{o,Adj}$) of 26°C decrease after applying the tool, showing a greater relative decrease with increased temperatures. *Figure 33* shows a clear reduction in overheating at higher temperatures. Uni-g 0.55 represents the initial duration diagram with a single g-value of the entire façade of the Reference Case equal to 0.55 and Ave-g 0.55 represents the duration diagram for the same façade, with distributed g-value for the façade according to the method.

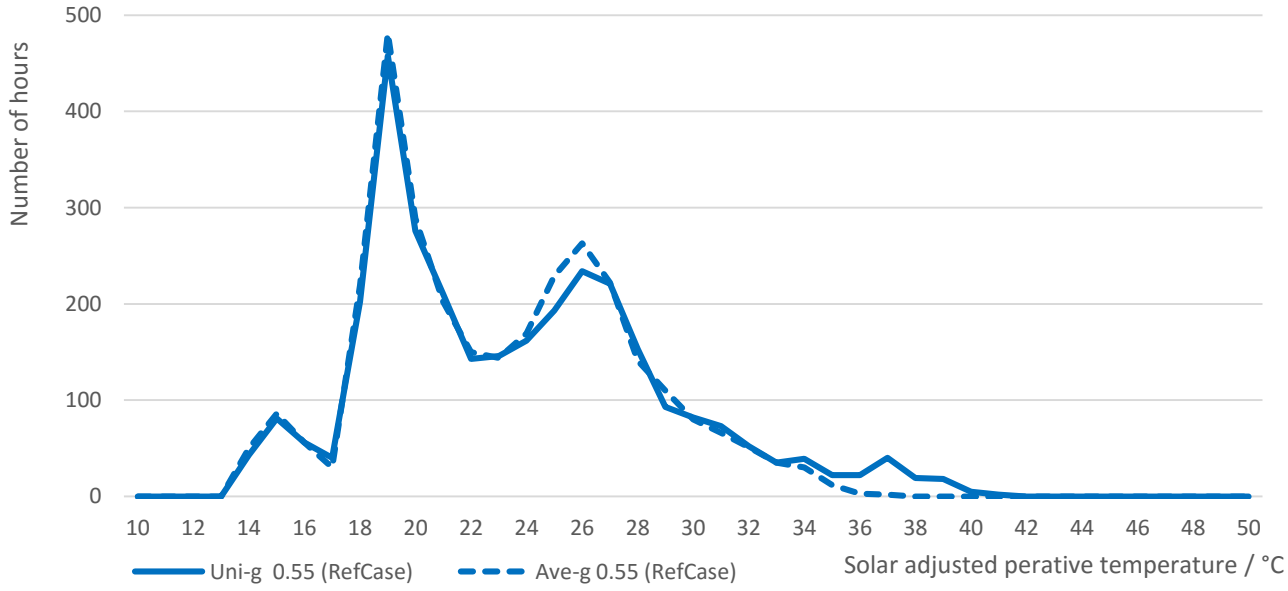

Figure 33: Annual $T_{o,Adj}$ duration diagram

All hours above the thresholds analyzed show improvements after applying the tool. The most significant advantage of the tool is apparent for overheating hours >35°C, showing an annual reduction of hours by 87%. Percentage improvement of number of hours with $T_{o,Adj}$ > 26°C, 28°C, 30°C are 9%, 19% and 32%, respectively, shown in *Figure 34*.

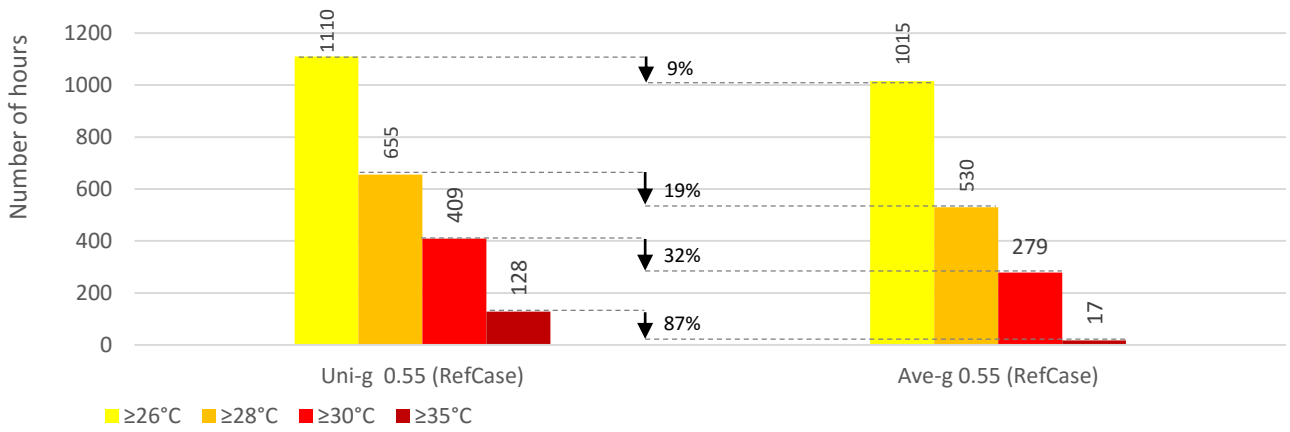

*Figure 34: Number of hours with $T_{o,Adj}$ > 26, 28, 30 and 35°C for the initial uniform glass g-*value *and redistributed g-*values *with average g-*value *of 0.55 for both cases.*

Time distribution

The functionality of the tool was observed on a weekly basis during three weeks of the year, namely an extremely hot, a typical and an extremely cold week relative Copenhagen climates conditions. The weather data from these weeks are taken from the .epw files. The cloud cover during the same periods is also analyzed to observe their effect on the tool. Cloud coverage is measured on a scale from 0-10, when zero indicated no clouds and ten is full coverage.

The extremely hot week in August, shown in *Figure 35*, is clear during most days, during which the temperature profiles before and after applying the method, look similar. However towards the end of the week, when the cloud cover increases, the peak temperatures decrease, and so does the efficiency of the tool. This correlation indicates the tools preferable functionality for periods with high solar irradiance.

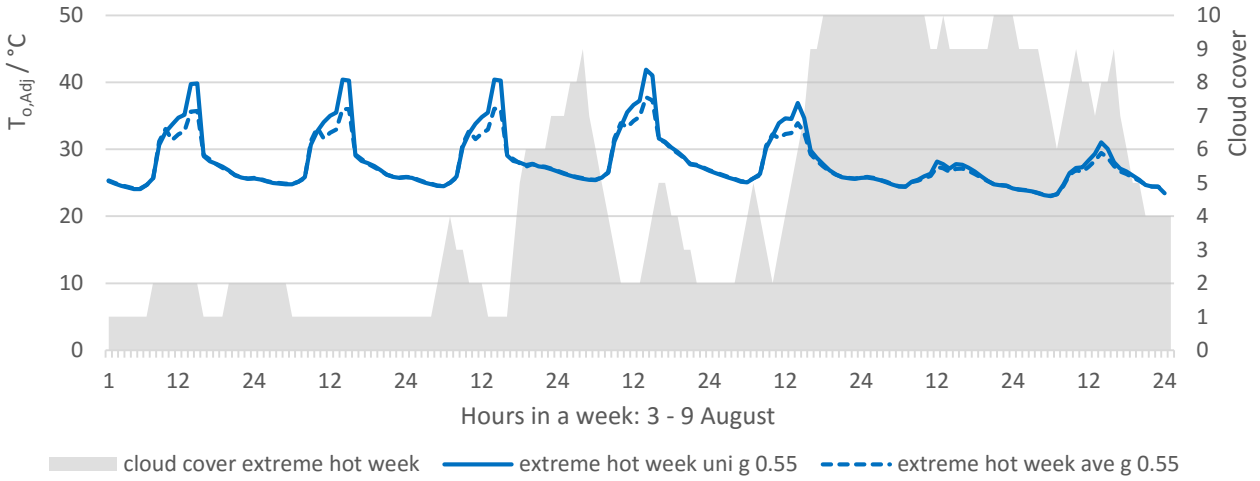

Figure 35: Extreme hot week 3-9/8, Copenhagen climate

A typical week in September, shows more encompassing cloud coverage throughout most of the week, allowing for marginal efficiency of the tool.

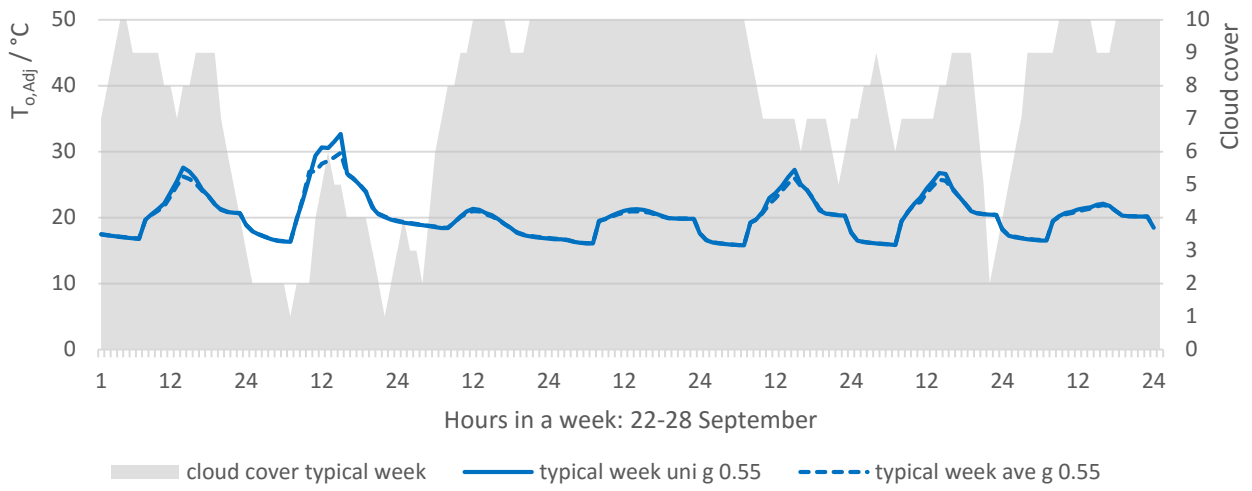

Figure 36: Typical week 22-28/9, Copenhagen climate

The extremely cold week, in February, displays clear conditions during the day for the first half of the week, with corresponding performance of the tool.

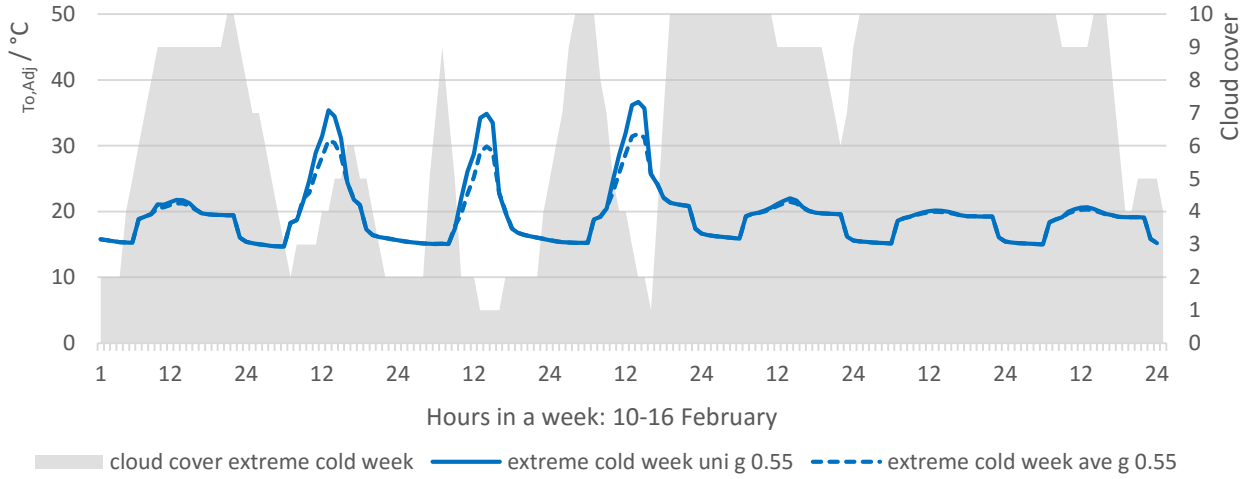

Figure 37: Extreme cold week 10-16/2, Copenhagen climate

Moreover, an hourly distribution of an annual simulation shows the reduction in overheating hours occur predominantly in the morning and early afternoon, shown by the light blue bars in *Figure 38*. This trend reflects the southerly orientation of the façade and the location of the analysis point, since it is mostly exposed to direct sun during the morning and early afternoon.

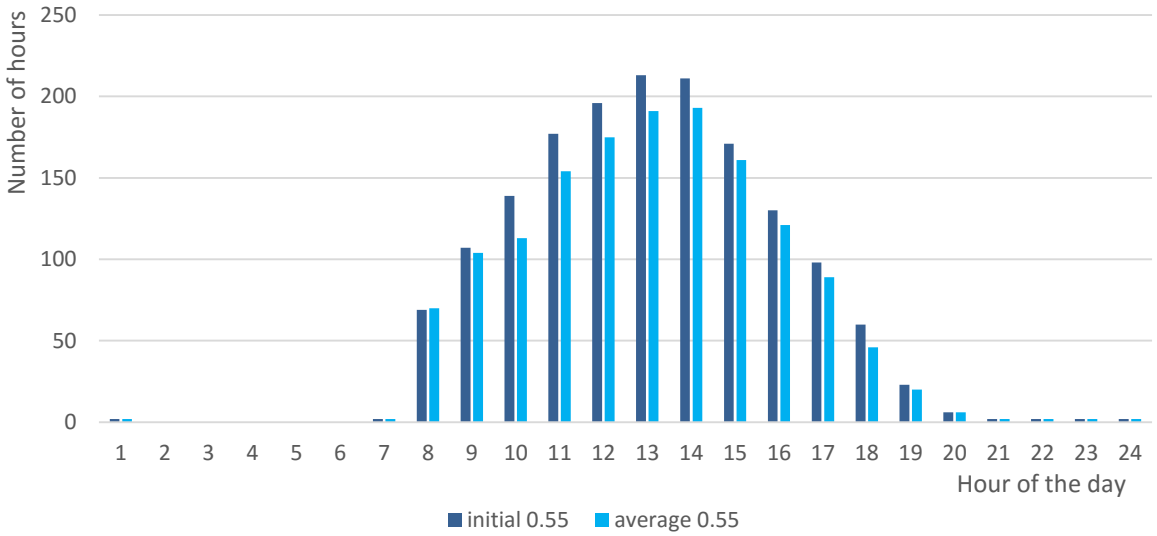

Figure 38: Hourly distribution of $T_{o,Adj}$ > 26°C on annual basis.

6.2 Sensitivity study

6.2.1 Frit geometry

The Reference Case geometry and input settings were tested with the addition of physical frit to the exterior of the glazing. Two types of frit patterns were tested; a uniform and non-uniform pattern. The frit was assumed to be opaque with an area corresponding to shading need of the glazing with a *g*-value of 0.7. The effectiveness of the method at improving thermal comfort in Point 0 was analyzed with the frit patterns and compared to the output for the Reference Case.

The tool output for the analyzed weather files is comprised of 1; Ray tracing module output, including re-distributed average *g*-values and uniform frit pattern, and 2; Thermal data output, including the numbers of hours above analyzed thresholds before and after applying the method.

6.2.1.1 Ray tracing module output

As can be seen in *Figure 39*, the uniform and non-uniform frit patterns correspond to the re-distributed average *g*-value of the Reference Case.

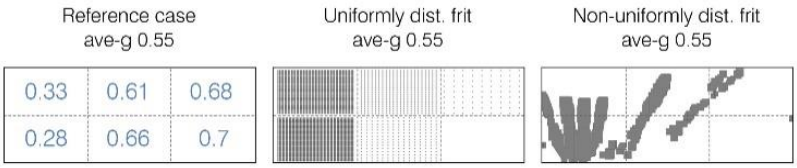

*Figure 39: Ray tracing module output of re-distributed g-*value*, uniform frit pattern and non-uniformly distributed frit based on positions of intersections.*

6.2.1.2 Thermal data output

Table 6 shows the number of hours (annually) above each threshold before (uni-g 0.55) and after (ave-g 0.55) applying the method to the comfort analysis of Point 0 for each frit pattern. The number of hours above all threshold show similar trends for both patterns, indicating a good translation of *g*-value to frit area.

*Table 6: Number of hours with $T_{o,Adj}$ > 26, 28, 30 and 35°C for the Reference Case with re-distributed g-*values *and two cases with physical geometry of frit in form of uniformly distributed frit and non-uniformly distributed frit.*

	Ref case uni g 0.55 /h	Ref case ave g 0.55 /h	Uniformly dist frit ave g 0.55 /h	Non-uniformly dist frit ave g 0.55 /h
≥26 °C	1110	1015	985	915
≥28 °C	655	530	516	451
≥30 °C	409	279	204	166
≥35 °C	128	17	52	48

The percentage differences between uni-g 0.55 and ave-g 0.55 for the Reference Case and both frit patterns are shown in *Figure 40*. The tool shows comparable potential for all methods of attaining the desired average g-value of 0.55. However, the case with re-distributed g-values performs best for high temperature threshold of 35°C, while both frit patterns are more effective for reducing temperatures of lower thresholds such as 26°C and 28°C. What is more, the non-uniformly distributed frit reduces the number of hours above all threshold slightly more than the uniform frit pattern.

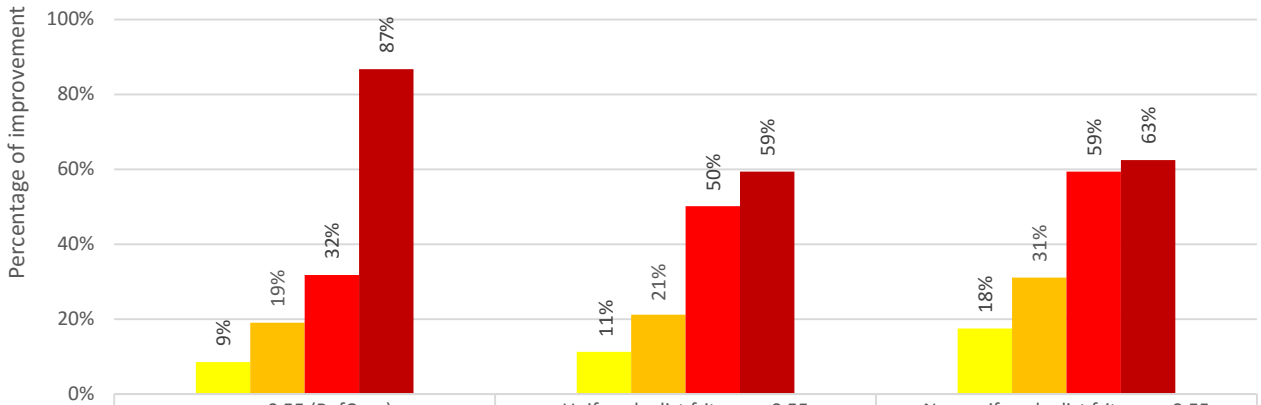

	ave g 0.55 (RefCase)	Uniformly dist frit ave g 0.55	Non-uniformly dist frit ave g 0.55
≥26 °C	9%	11%	18%
≥28 °C	19%	21%	31%
≥30 °C	32%	50%	59%
≥35 °C	87%	59%	63%

*Figure 40: Difference in number of hours with $T_{o,Adj}$ > 26, 28, 30 and 35°C for the Reference Case with re-distributed g-*values *and two cases with physical geometry of frit in form of uniformly distributed frit and non-uniformly distributed frit.*

6.2.2 Climate file

The Reference Case geometry and input settings were tested for two additional climates; Madrid and Abu Dhabi. The effectiveness of the method at improving thermal comfort in Point 0 was analyzed in the additional climates and compared to the output for the Reference Case climate of Copenhagen.

The tool output for the analyzed weather files is comprised of 1; Ray tracing module output, including re-distributed average *g*-values and uniform frit pattern, and 2; Thermal data output, including the numbers of hours above analyzed thresholds before and after applying the method.

6.2.2.1 Ray tracing module output

As can be seen in *Figure 41*, for the Madrid climate, the *g*-value is re-distributed to the bottom left corner of the façade, indicating a stronger need for shading there. In Abu Dhabi, the re-distribution of *g*-value on the façade is similar to Copenhagen.

*Figure 41: Ray tracing module output of re-distributed g-*value *and uniform frit pattern for Copenhagen (Reference Case), Madrid and Abu Dhabi.*

6.2.2.2 Thermal data output

Table 7 shows the number of hours (annually) above each threshold before (uni-g 0.55) and after (ave-g 0.55) applying the method to the comfort analysis for each climate. The number of hours above all thresholds are considerably higher in Abu Dhabi, indicating an acute overheating problem at Point 0 in this climate.

Table 7: Number of hours with $T_{o,Adj}$ > 26, 28, 30 and 35°C for cases with weather data for Copenhagen (Reference Case), Madrid and Abu Dhabi.

	Copenhagen uni-g 0.55 (RefCase) /h	Copenhagen ave-g 0.55 (RefCase) /h	Madrid uni-g 0.55 /h	Madrid ave-g 0.55 /h	Abu Dhabi uni-g 0.55 /h	Abu Dhabi ave-g 0.55 /h
≥26 °C	1110	1015	1766	1554	2974	2923
≥28 °C	655	530	1075	761	1542	1447
≥30 °C	409	279	706	391	867	804
≥35 °C	128	17	327	64	550	313

The percentage differences between uni-g 0.55 and ave-g 0.55 for each climate file are shown in *Figure 42*. The tool shows promising potential for all thresholds in Madrid and less probably prospective for Abu Dhabi.

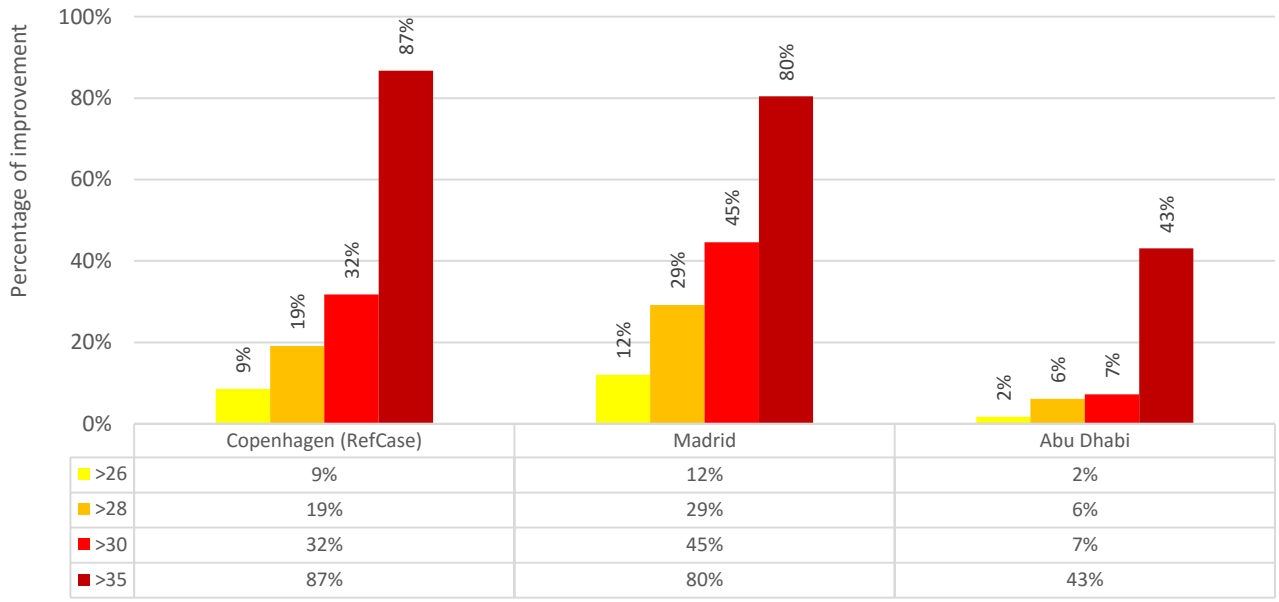

	Copenhagen (RefCase)	Madrid	Abu Dhabi
>26	9%	12%	2%
>28	19%	29%	6%
>30	32%	45%	7%
>35	87%	80%	43%

Figure 42: Difference in number of hours with $T_{o,Adj}$ > 26, 28, 30 and 35°C for cases with weather data for Copenhagen (Reference Case), Madrid and Abu Dhabi.

6.2.3 One point on the floor

Thus far, only Point 0 has been subject to thermal analysis in the analyzed zone. Hereby, the effectiveness of the method at improving thermal comfort in Point 1, 2, 3, 4 and Point 5 was tested and compared to the output for the Reference Case analysis of Point 0 for the climate of Copenhagen.

The tool output for the analyzed points is comprised of 1; Ray tracing module output, including re-distributed average *g*-value*s* and uniform frit pattern, and 2; Thermal data output, including the numbers of hours above analyzed thresholds before and after applying the method.

6.2.3.1 Ray tracing module output

As can be seen in *Figure 43*, the *g*-value distribution varies significantly depending on which point is chosen as analysis point.

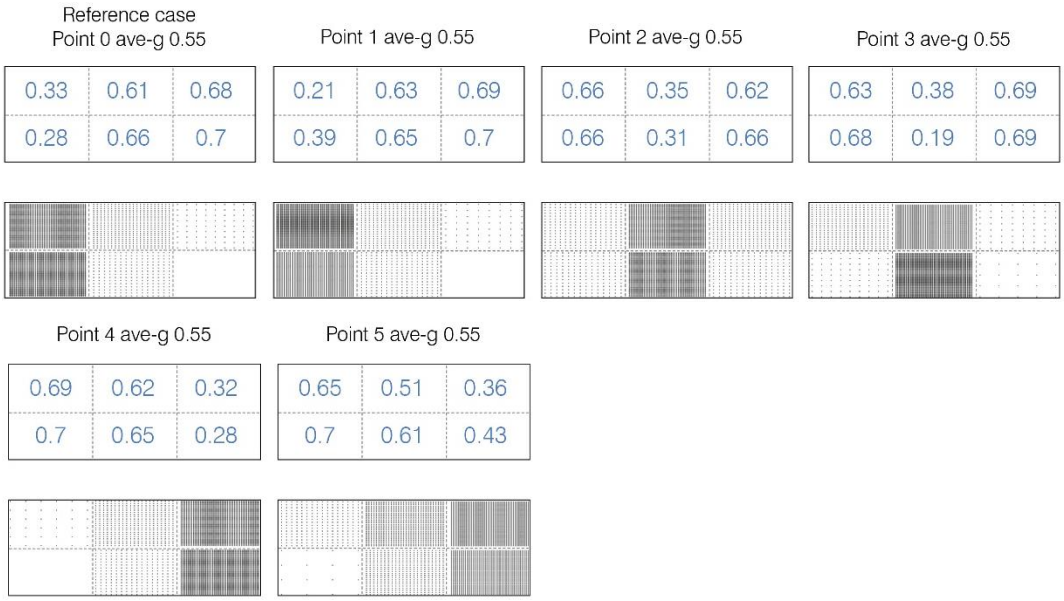

*Figure 43: Ray tracing module output of re-distributed g-*value *and uniform frit pattern for cases with six various locations of an analyzed point climate of Copenhagen.*

6.2.3.2 Thermal data output

Table 8 shows the number of hours (annually) above each threshold before (uni-g 0.55) and after (ave-g 0.55) applying the method to the comfort analysis for each point on the floor. The number of hours above all thresholds are considerably higher for Point 0, 2 and 4 which were located next to the glazed facade, indicating a greater overheating problem due to direct solar radiation.

Table 8: Number of hours with $T_{o,Adj}$ > 26, 28, 30 and 35°C for cases with six various locations of an analyzed point.

	Point0 uni-g 0.55 /h	Point0 ave-g 0.55 /h	Point1 uni-g 0.55 /h	Point1 ave-g 0.55 /h	Point2 uni-g 0.55 /h	Point2 ave-g 0.55 /h	Point3 uni-g 0.55 /h	Point3 ave-g 0.55 /h	Point4 uni-g 0.55 /h	Point4 ave-g 0.55 /h	Point5 uni-g 0.55 /h	Point5 ave-g 0.55 /h
≥26 °C	1110	1015	604	621	1154	1103	644	644	1045	946	671	678
≥28 °C	655	530	107	99	770	685	142	136	704	572	168	166
≥30 °C	409	279	33	19	524	440	54	43	496	361	72	67
≥35 °C	128	17	7	0	191	110	18	15	182	87	21	17

The percentage differences between uni-g 0.55 and ave-g 0.55 for all thresholds and for each point are shown in *Figure 44*. The tool shows more potential for improving comfort in spaces exposed to more direct sunlight.

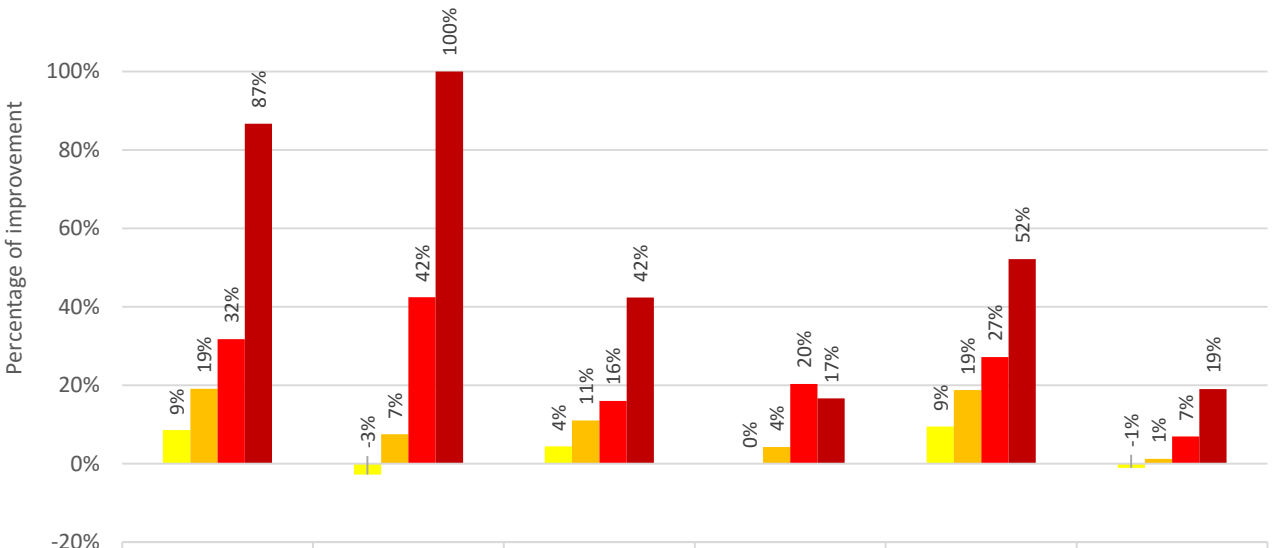

	Point0 (RefCase)	Point1	Point2	Point3	Point4	Point5
≥26 °C	9%	-3%	4%	0%	9%	-1%
≥28 °C	19%	7%	11%	4%	19%	1%
≥30 °C	32%	42%	16%	20%	27%	7%
≥35 °C	87%	100%	42%	17%	52%	19%

Figure 44: Difference in number of hours with $T_{o,Adj}$ > 26, 28, 30 and 35°C for cases with six various locations of an analyzed point.

6.2.4 Several points on the floor

Thus far, only Point 0 has been subject to thermal analysis. Hereby, the effectiveness of the method at improving thermal comfort in more than one point at a time, encompassing a larger analysis area, was tested and the resulting comfort for Point 0 was compared to the output for the Reference Case climate of Copenhagen.

The tool output for the analyzed points is comprised of 1; Ray tracing module output, including re-distributed average *g*-values and uniform frit pattern, and 2; Thermal data output, including the numbers of hours above analyzed thresholds before and after applying the method.

6.2.4.1 Ray tracing module output

Figure 45 shows how the average *g*-value distribution varies depending on how many points are simultaneously chosen as analysis points. It can clearly be seen that the larger the analyzed floor area, more wide spread the distribution becomes.

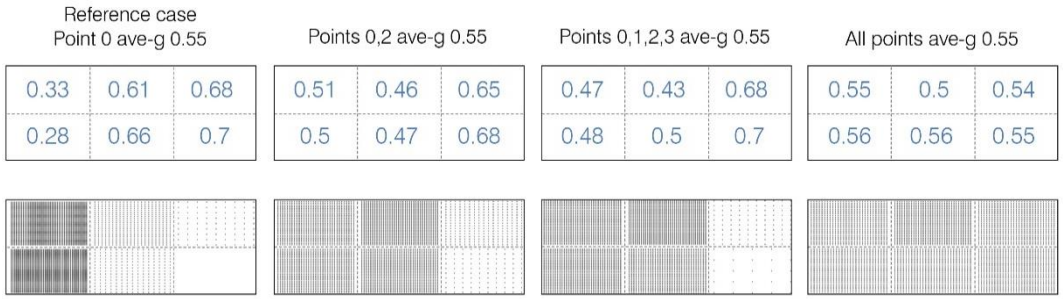

*Figure 45: Ray tracing module output of re-distributed g-*value *and uniform frit pattern for cases with point 0, points 0 and 2, points 0, 1, 2 and 3, and all points analyzed for climate of Copenhagen.*

6.2.4.2 Thermal data output

Table 9 shows the number of hours (annually) above each threshold after (ave-g 0.55) applying the method to the analysis for each combination of points on the floor. The results are compared to the Reference Case (uni-g 0.55).

Table 9: Number of hours with $T_{o,Adj}$ > 26, 28, 30 and 35°C for cases with point 0, points 0 and 2, points 0, 1, 2 and 3, and all points analyzed.

	Point 0 uni-g 0.55 (RefCase) /h	Point 0 ave-g 0.55 (RefCase) /h	Points 0+2 ave-g 0.55 /h	Points 0+1+2+3 ave-g 0.55 /h	All Points ave-g 0.55 /h
≥26 °C	1110	1015	1063	1053	1106
≥28 °C	655	530	609	588	650
≥30 °C	409	279	372	356	399
≥35 °C	128	17	107	95	131

The percentage differences between uni-g 0.55 and ave-g 0.55 for all thresholds and for each combination of points are shown in *Figure 46*. Increasing the spread of analysis points (i.e. increasing the analyzed floor area) shows a clear tendency of reducing the effectiveness of the tool. The results show that the case with only one analysis point, Point 0, experiences the highest thermal improvement with distributed *g*-value. The worst effect on thermal comfort in Point 0 occurs when all points are considered for the analysis, which even shows a degradation of comfort ≥ 35°C compared to the Reference Case.

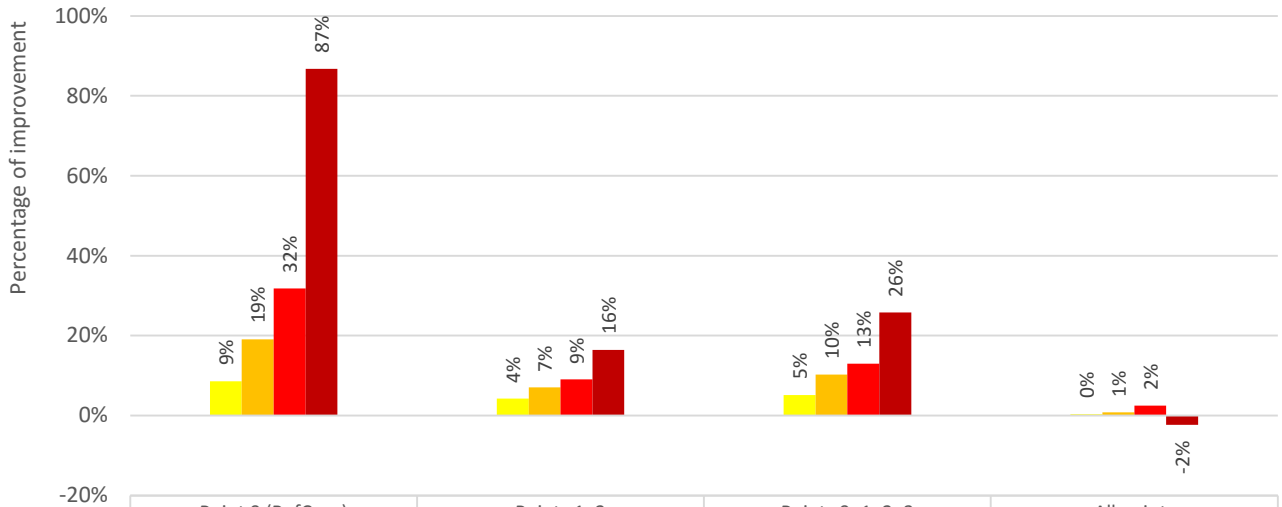

	Point 0 (RefCase)	Points 1+2	Points 0+1+2+3	All points
>26	9%	4%	5%	0%
>28	19%	7%	10%	1%
>30	32%	9%	13%	2%
>35	87%	16%	26%	-2%

Figure 46: Difference in number of hours with $T_{o,Adj}$ > 26, 28, 30 and 35°C for cases with point 0, points 0 and 2, points 0, 1, 2 and 3, and all points analyzed for Copenhagen climate.

6.2.5 Cooling threshold

The Reference Case geometry and input settings were tested for various cooling set point temperatures of the ideal load ventilation system. The effectiveness of the method at improving thermal comfort in Point 0 was analyzed at the cooling set points and compared to the output for the Reference Case set point temperature of 24°C.

The tool output for the analyzed set point temperatures is comprised of Thermal data output, including the numbers of hours above analyzed thresholds before and after applying the method for the Copenhagen climate.

6.2.5.1 Thermal data output

Table 10 shows the number of hours (annually) above each threshold before (uni-g 0.55) and after (ave-g 0.55) applying the method to the comfort analysis for each set point temperature.

Table 10: Number of hours with $T_{o,Adj}$ > 26, 28, 30 and 35°C for cases with cooling set points of 28°C, 26°C, 24°C (Reference Case), 22°C and the case with no cooling applied for Copenhagen climate.

	no conditioning uni-g 0.55 /h	no conditioning ave-g 0.56 /h	set pt 28 uni-g 0.55 /h	set pt 28 ave-g 0.55 /h	set pt 26 uni-g 0.55 /h	set pt 26 ave-g 0.55 /h	set pt 24 uni-g 0.55 (Ref case) /h	set pt 24 ave-g 0.55 (Ref case) /h	set pt 22 uni-g 0.55 /h	set pt 22 ave-g 0.55 /h
≥26 °C	1441	1436	1276	1236	1238	1189	1110	1015	769	632
≥28 °C	1361	1344	1030	980	911	822	655	530	479	341
≥30 °C	1245	1245	710	629	500	397	409	279	290	150
≥35 °C	1163	1151	215	115	172	53	128	17	85	0

The percentage differences between uni-g 0.55 and ave-g 0.55 for all thresholds and for each set point are shown in *Figure 47*. The tool shows almost no effect without conditioning of the space. Lowering the cooling set point temperature shows a clear tendency of increasing the effectiveness of the tool.

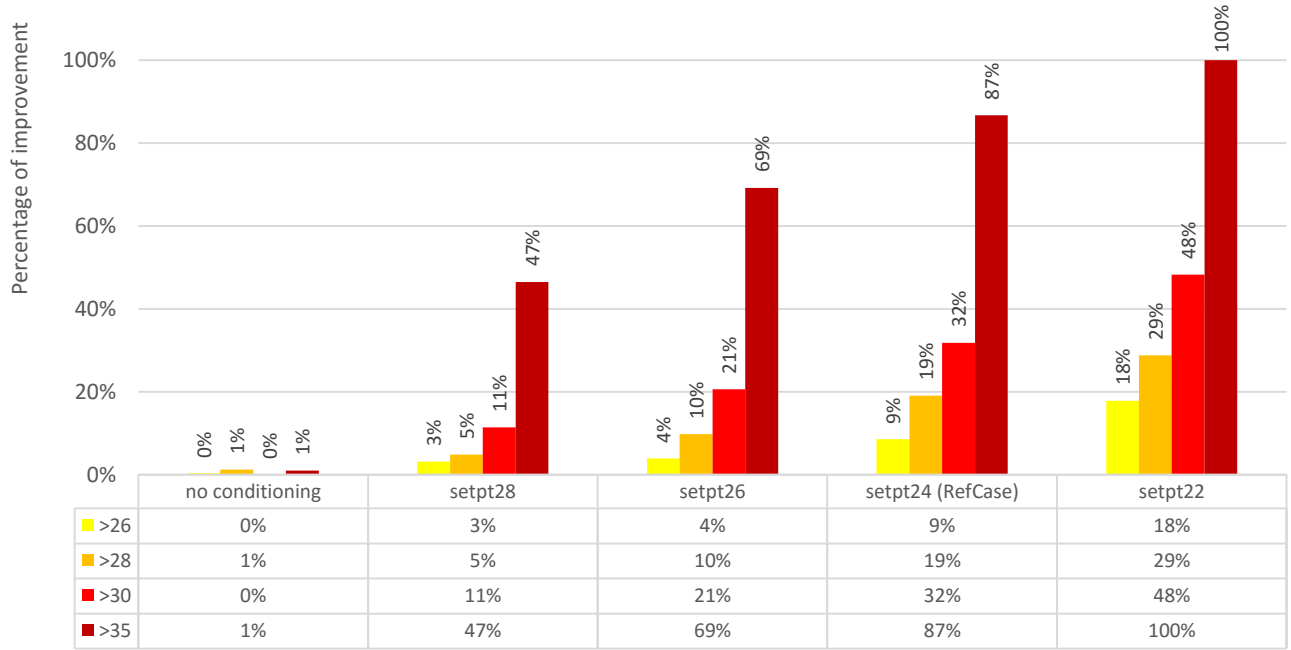

Figure 47: Difference in number of hours with $T_{o,Adj}$ > 26, 28, 30 and 35°C for cases with cooling set points of 28°C, 26°C, 24°C (Reference Case), 22°C, 21°C and the case with no cooling applied for Copenhagen climate.

6.2.6 Glazed façade grid

Thus far, the method has been tested only for glazed façade divided into the grid of 2·3 with glazing unit dimensions of 1.5 · 2.7 m. Hereby, the effectiveness of the method at improving thermal comfort for cases with façade grid of 2·2, 3·4 and 5·6 was tested. The dimensions of glazing units for the cases are 1.5 m · 4.0 m, 1.0 m · 2.0 m and 0.6 m · 1.7 m accordingly.

The tool output for the analyzed glazed façade grid is comprised of 1; Ray tracing module output, including re-distributed average *g*-values and uniform frit pattern, and 2; Thermal data output, including the numbers of hours above analyzed thresholds before and after applying the method for Copenhagen climate.

6.2.6.1 Ray tracing module output

Figure 48 shows how the average *g*-value distribution varies depending on how dense is the glazed façade grid. It can clearly be seen that the denser the grid, the more wide spread the distribution becomes. It can also be noticed, that the *g*-value is re-distributed to the middle left side of the façade, indicating a stronger need for shading there. Consequently, for the case with 3·4 grid, a shading need of the middle left grid exceeded the available area of the unit. Hereby, as described in *Section 4.3.4.3 Redistributed g-value definition*, the non-shaded glass *g*-value was lowered to 0.65 in order to compensate.

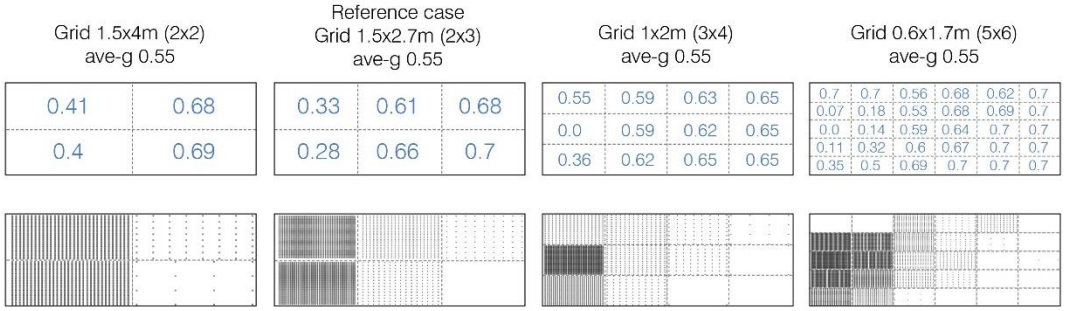

*Figure 48: Ray tracing module output of re-distributed g-*value *and uniform frit pattern for cases with grid dimensions of: 1.5 x 4.0 m (2x2), 1.0 x 2.0 m (3x4), 0.6 x 1.7 m (5x6) and 1.5mx2.7m (3x2) as the Reference Case for Copenhagen climate.*

6.2.6.2 Thermal data output

Table 11 displays the relative impact of the façade grid size on the number of hours above each threshold.

Table 11: Number of hours with $T_{o,Adj}$ > 26, 28, 30 and 35°C for cases with grid dimensions of: 1.5 x 4.0 m (2x2), 1.0 x 2.0 m (3x4), 0.6 x 1.7 m (5x6) and 1.5mx2.7m (3x2) as the Reference Case for Copenhagen climate.

	1.5x2.7 (3x2) uni-g 0.55 (RefCase) /h	1.5x4.0 (2x2) ave-g 0.55 /h	1.5x2.7 (2x3) ave-g 0.55 (RefCase) /h	1.0x2.0 (3x4) ave-g 0.55 /h	0.6x1.7 (5x6) ave-g 0.55 /h
≥26 °C	1110	1030	1015	947	908
≥28 °C	655	545	530	419	318
≥30 °C	409	311	279	166	85
≥35 °C	128	54	17	24	0

The percentage differences between uni-g 0.55 and ave-g 0.55 for all thresholds and for each of façade grid size are shown in *Figure 49*. A clear trend of reducing the number of hours above all thresholds by increasing the density of the grid can be observed.

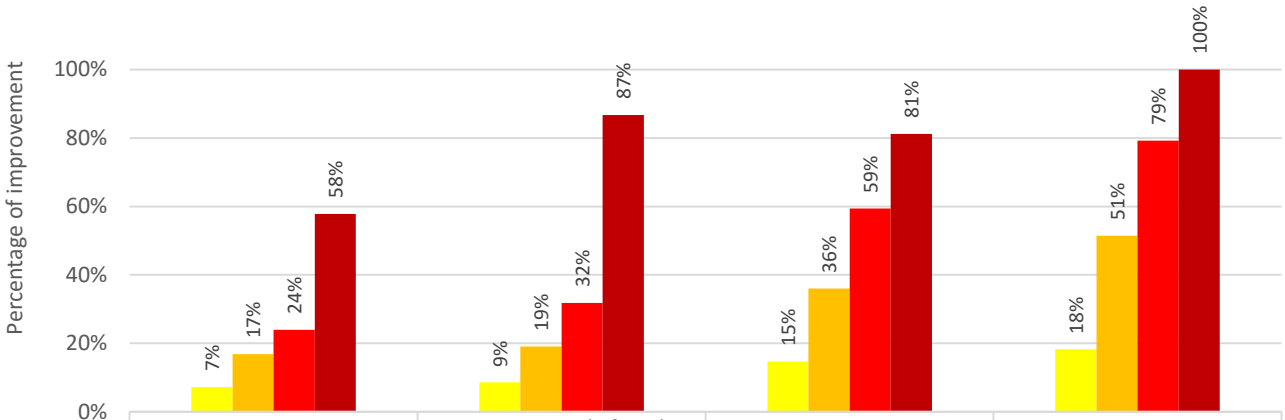

	2x2 ave g 0.55	3x2 ave g 0.55 (ref case)	4x3 ave g 0.55	6x5 ave g 0.55
≥26 °C	7%	9%	15%	18%
≥28 °C	17%	19%	36%	51%
≥30 °C	24%	32%	59%	79%
≥35 °C	58%	87%	81%	100%

Figure 49: Difference in number of hours with $T_{o,Adj}$ > 26, 28, 30 and 35°C for cases with grid dimensions of: 1.5 x 4.0 m (2x2), 1.0 x 2.0 m (3x4), 0.6 x 1.7 m (5x6) and 1.5mx2.7m (3x2) as the Reference Case for Copenhagen climate.

6.2.7 Factoring methods

The tool was tested for five additional factoring methods, described in *Section 4.4.2.7 Factoring methods*:

- Factors 1
- Factors 0.2-1
- Factors 0.4-1
- Factors 0.6-1
- Factors 0.8-1

The effectiveness of the method at improving thermal comfort in Point 0 was analyzed for each of the factoring methods and compared to the output for the Reference Case for which all factors between 0-1 were used.

The tool output for the analyzed factoring methods is comprised of 1. Ray tracing module output, including re-distributed average *g*-values, uniform frit pattern and ray-traced intersections, and 2. Thermal data output, including the numbers of hours above analyzed thresholds for the Reference case and five additional factoring methods for Copenhagen climate.

6.2.7.1 Ray tracing module output

Figure 50 shows how the average *g*-value distribution varies depending on what type of factoring intervals are applied. The largest differentiation of g-values were achieved with the factoring methods of 0.6-1 and 0.8-1, while case with all factors set to 1 resulted in the least diverse g-values on the façade.

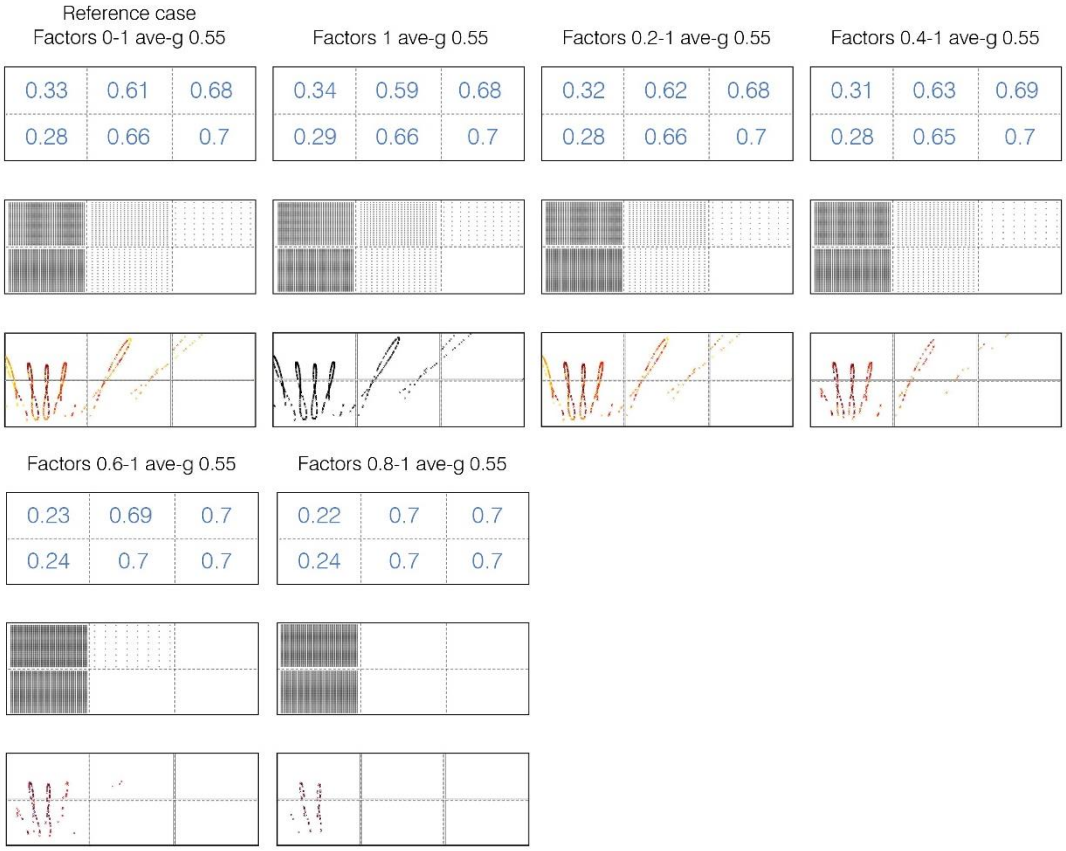

*Figure 50: Ray tracing module output of re-distributed g-*value*, uniform frit pattern and ray traced intersections for six types of factoring methods.*

6.2.7.2 Thermal data output

The two graphs in *Figure 51* portray how the monthly distribution of solar overheating factors is effected by the choice of factoring method. Two factoring methods were tested: Factors 0-1 (Reference case) and Factors 1. The right pie chart represents the Reference Case with factors between 0-1 and shows slightly higher relative importance of each solar overheating factor from July to August than the case with all factors of 1, represented by the left pie chart. Consequently, the case with all factors set to 1 reveals slightly higher relative importance of solar overheating factors from February to May.

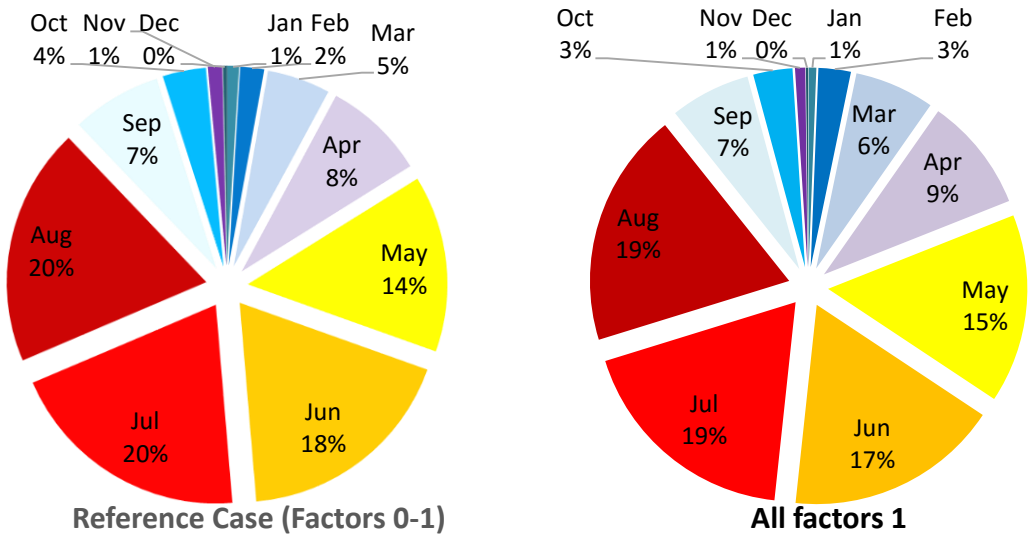

Figure 51: Monthly distribution of solar overheating factors for case with applied factors between 0-1 (Reference Case) and case with all applied factors equal to 1.

Table 12 shows the number of hours (annually) above each threshold for cases after (ave-g 0.55) applying the method with each of the tested factors intervals. The results are compared with the results for the Reference case before (uni-g 0.55) the application of the method.

Table 12: Number of hours with $T_{o,Adj}$ > 26, 28, 30 and 35°C for cases with factors of 1, factors 0.2-1, factors 0.4-, factors 0.6-1, factors 0.8-1 and factors between 0-1 (Reference Case).

	Uni-g 0.55 (RefCase) /h	Factors 0-1 Ave-g 0.55 (RefCase) /h	Factors 1 Ave-g 0.55 /h	Factors 0.2-1 Ave-g 0.55 /h	Factors 0.4-1 Ave-g 0.55 /h	Factors 0.6-1 Ave-g 0.55 /h	Factors 0.8-1 Ave-g 0.55 /h
≥26 °C	1110	1015	1023	1013	1012	988	988
≥28 °C	655	530	539	529	527	488	488
≥30 °C	409	279	288	277	275	246	244
≥35 °C	128	17	22	11	11	2	2

Figure 52 shows the effect of the tested factoring methods on number of hours with $T_{o,Adj}$ > 26, 28, 30 and 35°C. In general, the choice of the principle how the intersection points are factored, shows a limited impact on the effectiveness of the tool. However, the lowest advantage of the tool can be noticed when all factors are set to 1, and as such no factoring method is applied.

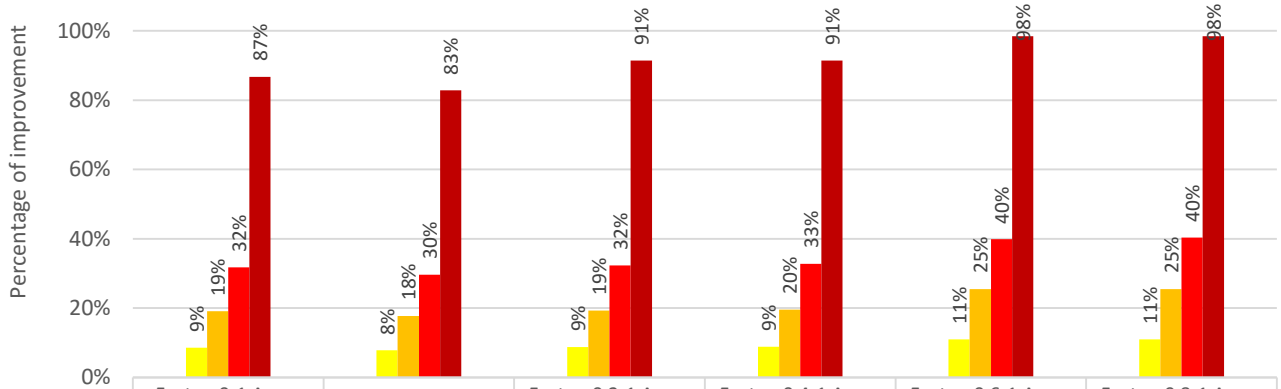

	Factors0-1 Ave-g 0.55 (RefCase)	Factors1 Ave-g 0.55	Factors0.2-1 Ave-g 0.55	Factors0.4-1 Ave-g 0.55	Factors0.6-1 Ave-g 0.55	Factors0.8-1 Ave-g 0.55
>26	9%	8%	9%	9%	11%	11%
>28	19%	18%	19%	20%	25%	25%
>30	32%	30%	32%	33%	40%	40%
>35	87%	83%	91%	91%	98%	98%

Figure 52: Difference in number of hours with $T_{o,Adj}$ > 26, 28, 30 and 35°C for cases with factors of 1, factors 0.2-1, factors 0.4-, factors 0.6-1, factors 0.8-1 and factors between 0-1 (Reference Case).

6.2.8 Orientation

Thus far, the geometry with glazed façade oriented to the South has been subject to thermal analysis. Hereby, the effectiveness of the method at improving thermal comfort in spaces with glazed façade oriented to the East and to the West was tested.

The tool output for the analyzed glazed façade orientation is comprised of 1; Ray tracing module output, including re-distributed average *g*-values and uniform frit pattern, and 2; Thermal data output, including the numbers of hours above analyzed thresholds before and after applying the method for Copenhagen climate.

6.2.8.1 Ray tracing module output

As can be seen in *Figure 53*, for the eastern orientation, the g-value is re-distributed to the bottom left corner of the façade, indicating stronger need for shading there. For the western orientation, the lower g-values are also re-distributed to the bottom left corner, however the shading need applies to larger number of the glazing units.

*Figure 53: Ray tracing module output of re-distributed g-*value *and uniform frit pattern for south- (Reference Case), east- and west-oriented cases.*

6.2.8.2 Thermal data output

Table 13 shows the number of hours (annually) above each threshold before (uni-g 0.55) and after (ave-g 0.55) applying the method to the comfort analysis for each orientation case. The number of hours above all thresholds are considerably higher for the space with southerly oriented glazed façade than for spaces with easterly or westerly oriented glazed facades.

Table 13: Number of hours with $T_{o,Adj}$ > 26, 28, 30 and 35°C for south (Reference Case), east and west oriented cases.

	South Uni-g 0.55 (RefCase) /h	South Ave-g 0.55 (RefCase) /h	East Uni-g 0.55 /h	East Ave-g 0.55 /h	West Uni-g 0.55 /h	West Ave-g 0.55 /h
≥26°C	1110	1015	866	525	746	561
≥28°C	655	530	351	97	417	290
≥30°C	409	279	170	47	291	140
≥35°C	128	17	21	7	93	18

Figure 54 displays the relative impact of the façade orientation on the number of hours above each threshold. Clearly, the southern and western orientations show biggest advantage of the method for high $T_{o,Adj}$ threshold of 35°C, while eastern orientation performs best for threshold of 28°C.

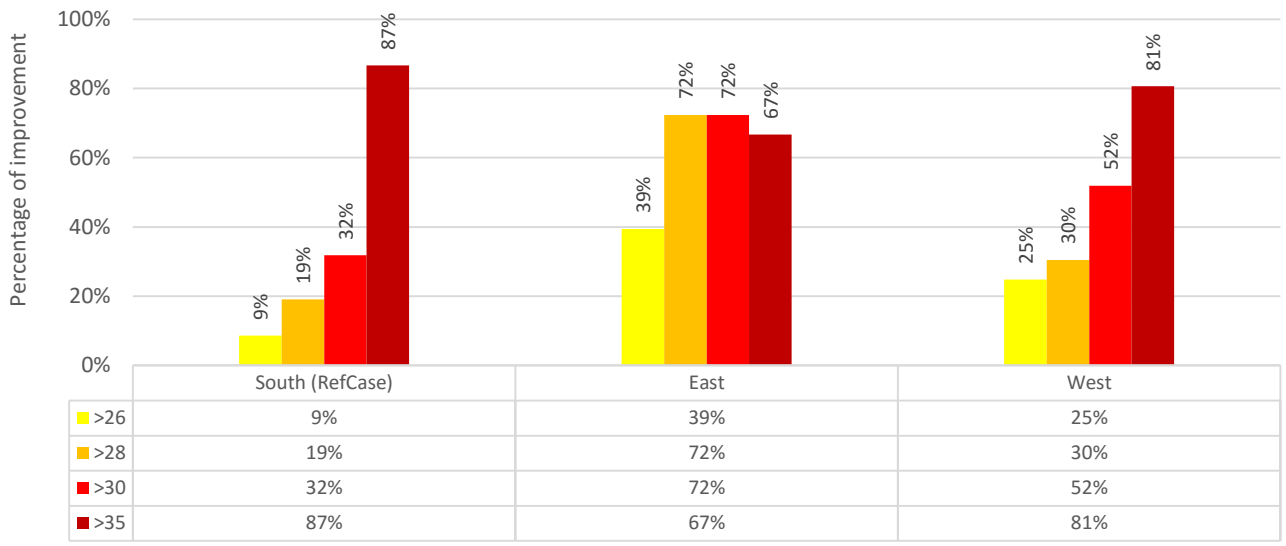

	South (RefCase)	East	West
>26	9%	39%	25%
>28	19%	72%	30%
>30	32%	72%	52%
>35	87%	67%	81%

Figure 54: Difference in number of hours with $T_{o,Adj}$ > 26, 28, 30 and 35°C for south (Reference Case), east and west oriented cases for Copenhagen climate.

As shown on a weekly time distribution graph in *Figure 55*, a clear reduction of peak operative temperatures on a sunny and moderately cloudy afternoon is noticeable for west orientation. As expected and shown in *Figure 56*, the east-oriented case displays a potential of reducing peak operative temperatures on sunny days before noon. Moreover, the results shows a significant reduction of overheating hours on cloudy days for east-oriented case, most likely due to high impact of diffuse radiation on perceived operative temperatures.

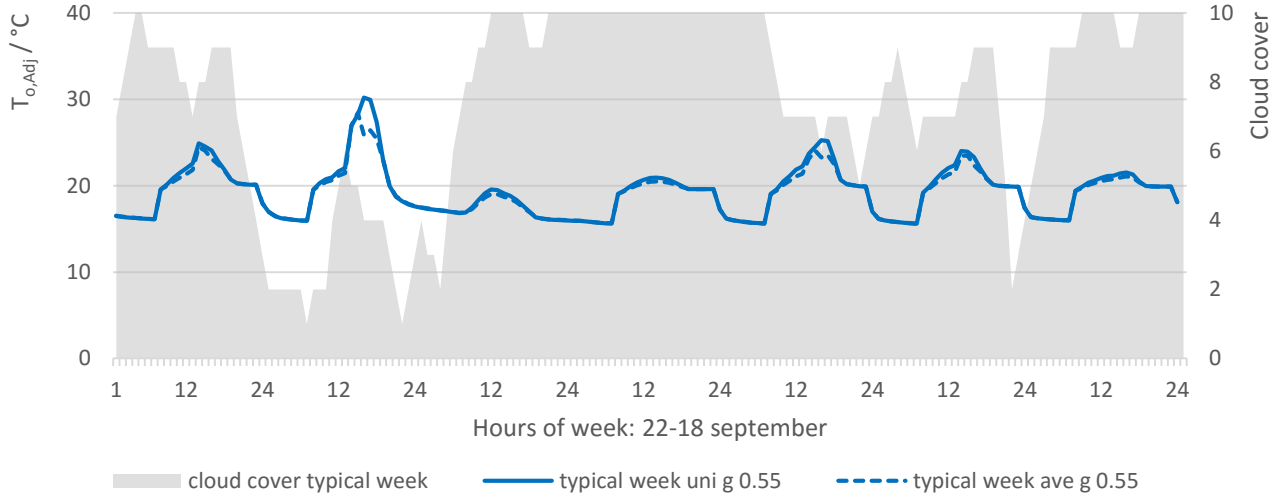

Figure 55: $T_{o,Adj}$ distribution in typical week for west orientation

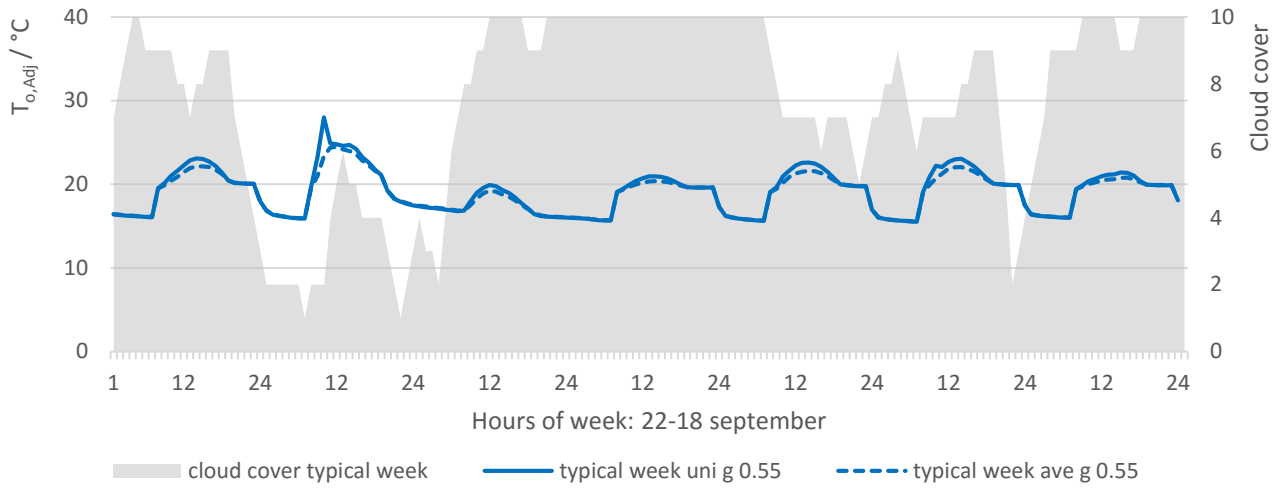

Figure 56: $T_{o,Adj}$ distribution in typical week for east orientation.

6.2.9 Glazing ratio

The Reference Case geometry and input settings were tested for four additional glazing to floor ratios:

- GFR 7.5 %
- GFR 15 %
- GFR 30 %
- GFR 80 %

The effectiveness of the method at improving thermal comfort in Point 0 was analyzed for the additional glazing cases and compared to the output for the Reference Case with the GWR of 60 %.

The tool output for the analyzed glazing ratios is comprised of 1; Ray tracing module output, including re-distributed average *g*-values and uniform frit pattern, and 2; Thermal data output, including the numbers of hours above analyzed thresholds before and after applying the method for Copenhagen climate.

6.2.9.1 Ray tracing module output

As can be seen in *Figure 57*, the *g*-value distribution varies significantly depending on which glazing ratio is tested. It can also be noticed, that for the case with GWR of 80% and glazing on the façade and the roof simultaneously, the *g*-values are lowered only on the façade, indicating that no shading is needed on the roof.

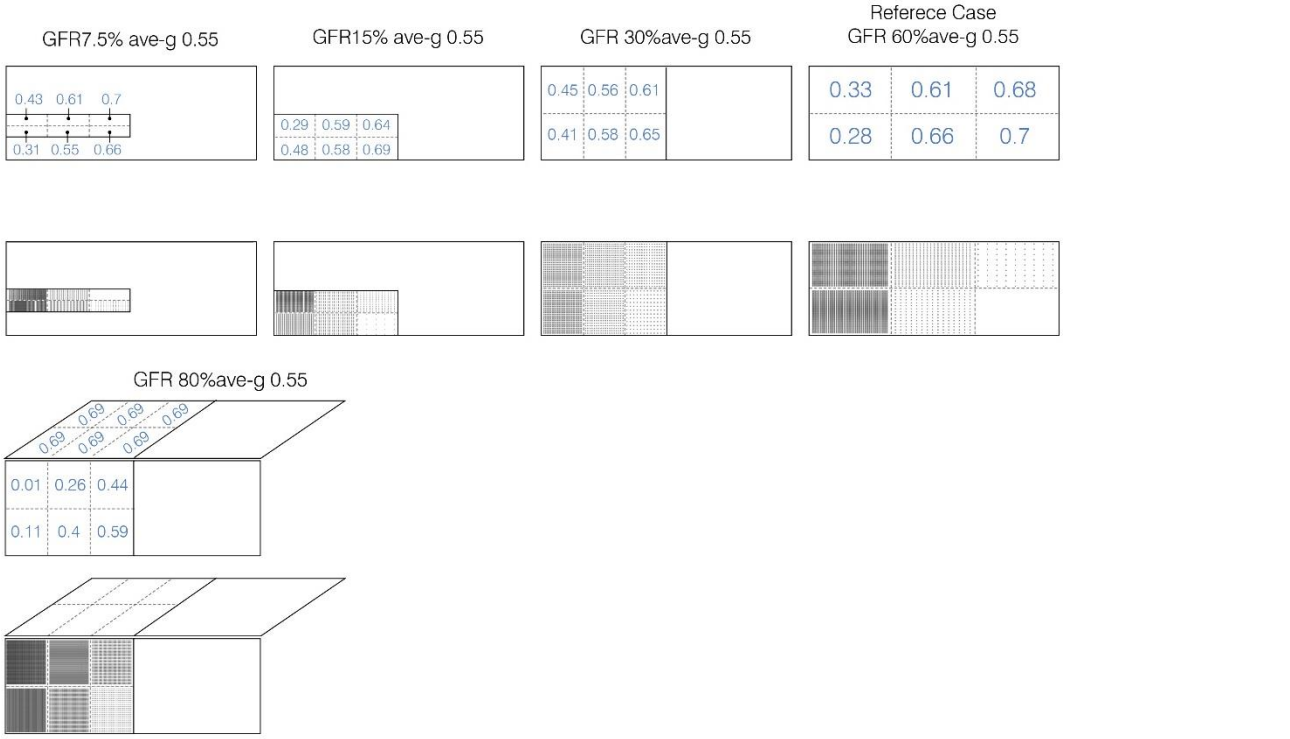

*Figure 57: Output of re-distributed g-*value *and uniform frit pattern for the cases with GWR 7.5%, GWR 15%, GWR 30%, GWR 80% and GWR 60% (Reference Case).*

6.2.9.2 Thermal data output

Testing different glazing to floor ratios indicates that the method performs better for cases with lower percentage of fenestration. However, it is important to note that location of a window on a façade might have a high impact on the result and thus each case should be treated individually.

Table 14 shows the number of hours (annually) above each threshold before (uni-g 0.55) and after (ave-g 0.55) applying the method to the comfort analysis for each glazing ratio. The number of hours above all thresholds are considerably higher for cases with higher ratios of glazing.

Table 14: Number of hours with $T_{o,Adj}$ > 26, 28, 30 and 35°C for the cases with GWR 7.5%, GWR 15%, GWR 30%, GWR 80% and GWR 60% (Reference Case).

	GFR7.5% Uni-g 0.55 /h	GFR7.5% Ave-g 0.55 /h	GFR15% Uni-g 0.55 /h	GFR15% Ave-g 0.55 /h	GFR30% Uni-g 0.55 /h	GFR30% Ave-g 0.55 /h	GFR60% Uni-g 0.55 (RefCase) /h	GFR60% Ave-g 0.55 (RefCase) /h	GFR80% Uni-g 0.55 /h	GFR80% Ave-g 0.55 /h
≥26	64	54	122	104	560	527	1110	1015	1210	1167
≥28	42	16	58	32	289	279	655	530	892	833
≥30	26	4	40	2	190	166	409	279	561	489
≥35	0	0	2	0	55	10	128	17	174	15

The results in *Figure 58* show that the best performance of the method was achieved for glazing ratio of 15%. What is more, for cases with lower glazing ratios, the method was also preferred for lower thresholds of operative temperatures such as 26°C and 28°C.

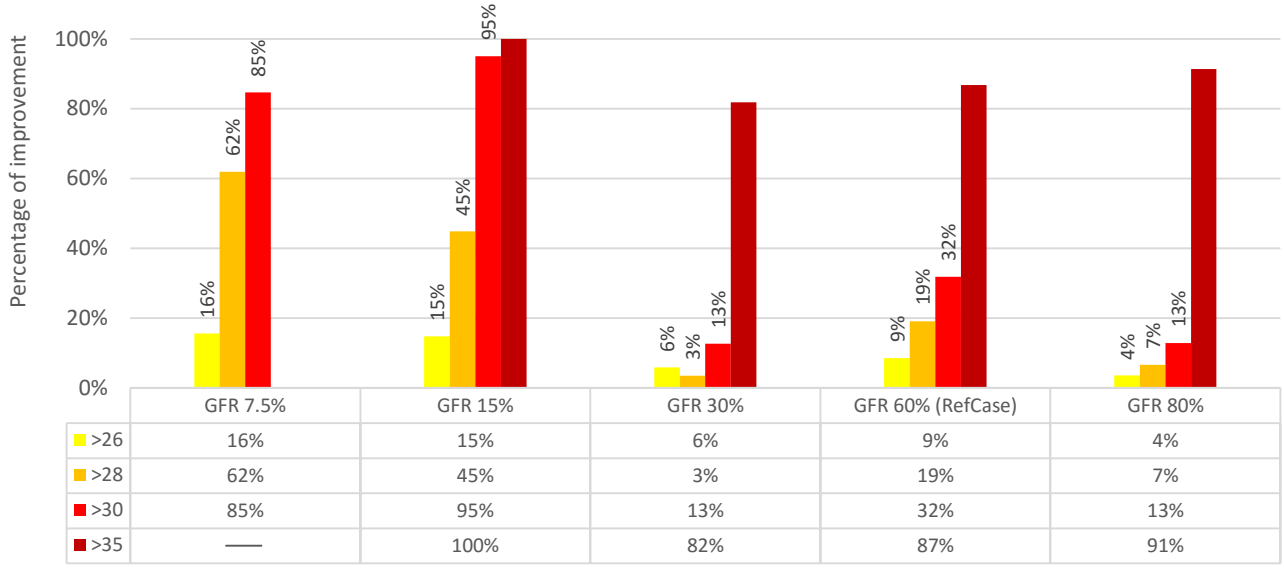

Figure 58: Difference in number of hours with $T_{o,Adj}$ > 26, 28, 30 and 35°C for the cases with GWR 7.5%, GWR 15%, GWR 30%, GWR 80% and GWR 60% (Reference Case) for Copenhagen climate.

6.2.10 Average *g*-value of glass

The method was tested for three additional cases with different average *g*-values of glass:

- average *g*-value of 0.65 (ave-*g* 0.65)
- average *g*-value of 0.45 (ave-*g* 0.45)
- average *g*-value of 0.35 (ave-*g* 0.35)

The effectiveness of the method at improving thermal comfort in Point 0 was analyzed for the additional cases and compared to the output for the Reference Case with average glass *g*-value of 0.55.

The tool output for the analyzed cases of average glass *g*-value is comprised of 1. Ray tracing module output, including re-distributed average *g*-values and uniform frit pattern, and 2. Thermal data output, including the numbers of hours above analyzed thresholds before and after applying the method for Copenhagen climate.

6.2.10.1 Ray tracing module output

As can be seen in *Figure 59*, the lower the average glass g-value, the wider spread the distribution becomes.

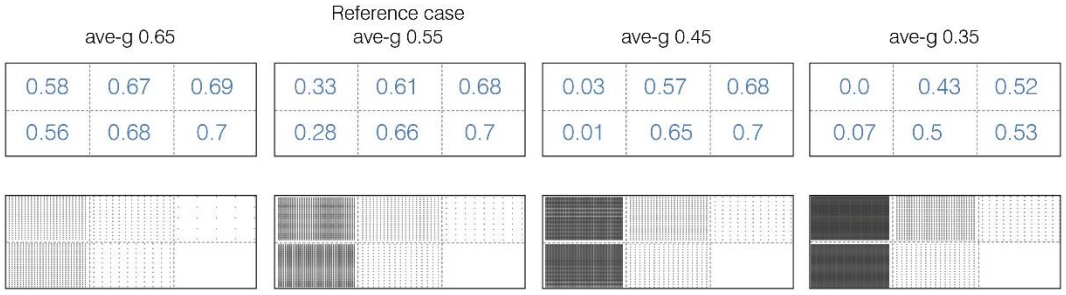

*Figure 59: Output of re-distributed g-*value *and uniform frit pattern for the cases with average g-*value *of 0.65, 0.55 (Reference Case), 0.45 and 0.35.*

6.2.10.2 Thermal data output

By changing the average *g*-value of glazed façade a clear trend of higher advantage of the method for cases with lower average *g*-value can be noticed. In other words, cases with less extensive overheating problems are more likely to benefit from the method.

Table 15 shows the number of hours (annually) above each threshold before (uni-g) and after (ave-g) applying the method to the comfort analysis for each average glass *g*-value case. The number of hours above all thresholds are considerably higher for a case with highest average glass *g*-value of 0.65.

*Table 15: Number of hours with $T_{o,Adj}$ > 26, 28, 30 and 35°C for the cases with average g-*value *of 0.65, 0.55 (Reference Case), 0.45 and 0.35.*

	Uni-g 0.55 (RefCase) /h	Ave-g 0.55 (RefCase) /h	Uni-g 0.65 /h	Ave-g 0.65 /h	Uni-g 0.45 /h	Ave-g 0.45 /h	Uni-g 0.35 /h	Ave-g 0.35 /h
≥26 °C	1110	1015	1317	1280	835	620	651	145
≥28 °C	655	530	929	857	423	175	318	25
≥30 °C	409	279	574	523	252	36	165	0
≥35 °C	128	17	216	178	43	0	2	0

As displayed in *Figure 60*, the case with average *g*-value of 0.35 displays a potential of reducing the overheating risk of 651 hours with $T_{o,Adj}$ over 26°C by 78%. Moreover, the results clearly show that the method is more favorable to eliminate high ranges of $T_{o,Adj,}$ such as 35°C.

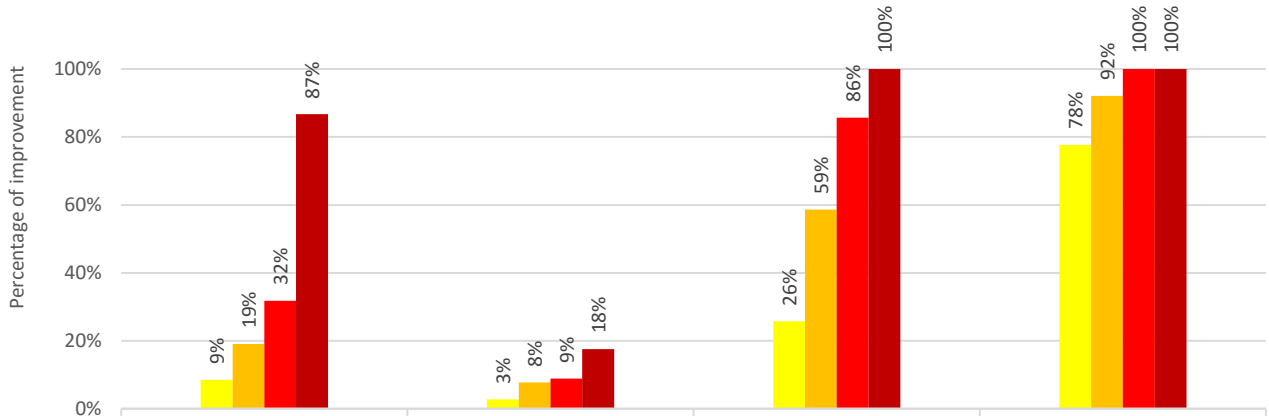

	Ave-g 0.55 (RefCase)	Ave-g 0.65	Ave-g 0.45	Ave-g 0.35
≥26°C	9%	3%	26%	78%
≥28°C	19%	8%	59%	92%
≥30°C	32%	9%	86%	100%
≥35°C	87%	18%	100%	100%

*Figure 60: Difference in number of hours with $T_{o,Adj}$ > 26, 28, 30 and 35°C for the cases with average g-*value *of 0.65, 0.55 (Reference Case), 0.45 and 0.35 for Copenhagen climate.*

6.2.11 Analysis period

Thus far, only the annual basis has been subject to thermal analysis of the Reference case. Hereby, the effectiveness of the method at improving thermal comfort was tested for four more periods:

- one season (summer),
- one month (August),
- one week (in August) and
- one day (2nd August)

The effectiveness of the method at improving thermal comfort in Point 0 was analyzed for the additional periods and compared to the output for the Reference Case with annual analysis period.

The tool output for the analyzed periods is comprised of 1; Ray tracing module output, including re-distributed average *g*-values and uniform frit pattern, and 2; Thermal data output, including the numbers of hours above analyzed thresholds before and after applying the method for Copenhagen climate.

6.2.11.1 Ray tracing module output

Figure 61 shows how the average *g*-value distribution varies depending on the chosen analysis period. It can clearly be seen that the shorter analysis period, the wider spread of g-value distribution becomes.

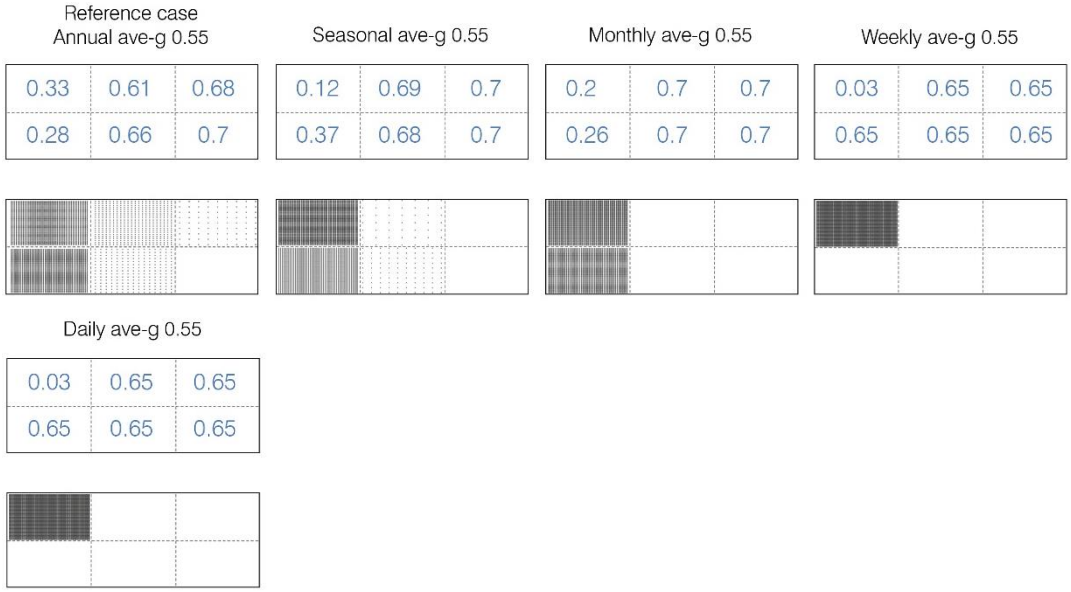

*Figure 61: Ray tracing module output of re-distributed g-*value *and uniform frit pattern for the cases with annual (Reference Case), seasonal (summer), monthly (August), weekly (3.-9. August) and daily (2.August) analysis period.*

6.2.11.2 Thermal data output

Table 16 shows the number of hours (annually) above each threshold before (uni-g 0.55) and after (ave-g 0.55) applying the method to the comfort analysis for each analysis period for Copenhagen climate.

Table 16: Number of hours with $T_{o,Adj}$ > 26, 28, 30 and 35°C for the cases with annual (Reference Case), seasonal (summer), monthly (August), weekly (3.-9. August) and daily (2.August) analysis period.

	Annual uni-g 0.55 (RefCase) /h	Annual ave-g 0.55 (RefCase) /h	Season uni-g 0.55 /h	Season ave-g 0.55 /h	Month uni-g 0.55 /h	Month ave-g 0.55 /h	Week uni-g 0.55 /h	Week ave-g 0.55 /h	Daily uni-g 0.55 /h	Daily ave-g 0.55 /h
≥26 °C	1110	1015	629	592	213	194	58	58	10	10
≥28 °C	655	530	339	261	128	109	46	46	9	9
≥30 °C	409	279	184	96	78	51	33	25	6	4
≥35 °C	128	17	52	1	23	2	10	0	2	0

As displayed in *Figure 62,* changing the period for which the simulation is run, shows a tendency to eliminate higher temperatures more effectively with shorter analysis periods. The effect of the method becomes clearer.

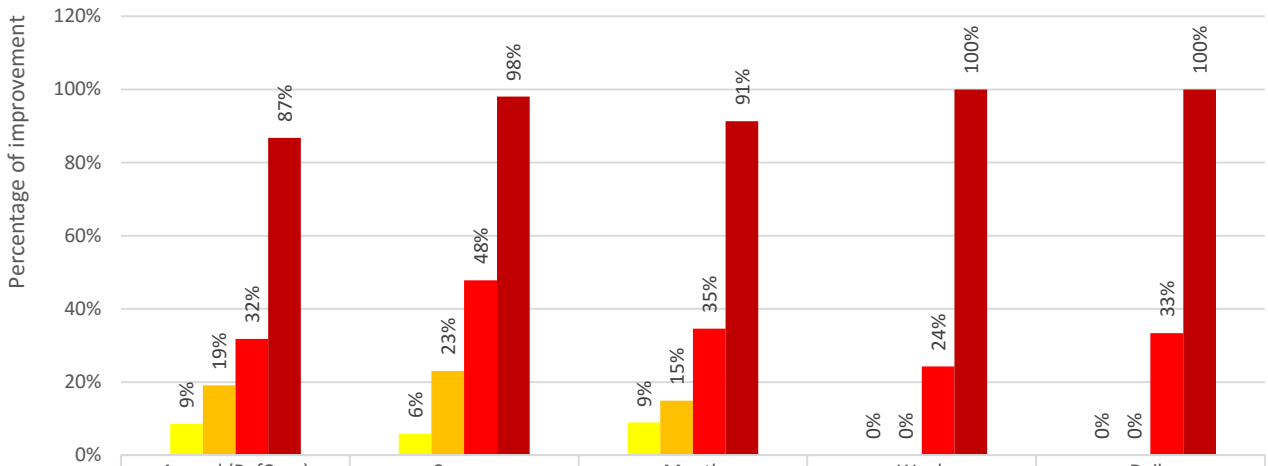

	Annual (RefCase)	Season	Month	Week	Daily
≥26 °C	9%	6%	9%	0%	0%
≥28 °C	19%	23%	15%	0%	0%
≥30 °C	32%	48%	35%	24%	33%
≥35 °C	87%	98%	91%	100%	100%

Figure 62: Difference in number of hours with $T_{o,Adj}$ > 26, 28, 30 and 35°C for the cases with annual (Reference Case), seasonal (summer), monthly (August), weekly (3.-9. August) and daily (2.August) analysis period for Copenhagen climate.

6.2.12 Saving potential

The thermal requirement of the case was assumed adjusted to a fixed uniform glass *g*-value, in this case 0.55. Hereby, the thermal performance difference between the uniform and the average glass g-value distribution can be "compensated" by increasing the average *g*-value while maintaining thermal performance in the range of uniform glass g-value of 0.55 scenario. Savings can be reflected in the form of higher light levels or lower glazing costs (assuming that glazing with higher *g*-value is less expensive).

The method was tested for four additional cases with slightly higher average *g*-values than the Reference case:

- average *g*-value of 0.56 (ave-*g* 0.56)
- average *g*-value of 0.58 (ave-*g* 0.58)
- average *g*-value of 0.60 (ave-*g* 0.60)
- average *g*-value of 0.62 (ave-*g* 0.62)

The effectiveness of the method at improving thermal comfort in Point 0 was analyzed for the additional cases and compared to the output for the Reference Case with average glass *g*-value of 0.55.

The tool output for the analyzed saving potential is comprised of 1; Ray tracing module output, including re-distributed average *g*-values and 2; Thermal data output, including the numbers of hours above analyzed thresholds before and after applying the method for Copenhagen climate.

6.2.12.1 Ray tracing module output

Figure 63 shows how the average *g*-value distribution varies depending on the desired average glass g-value.

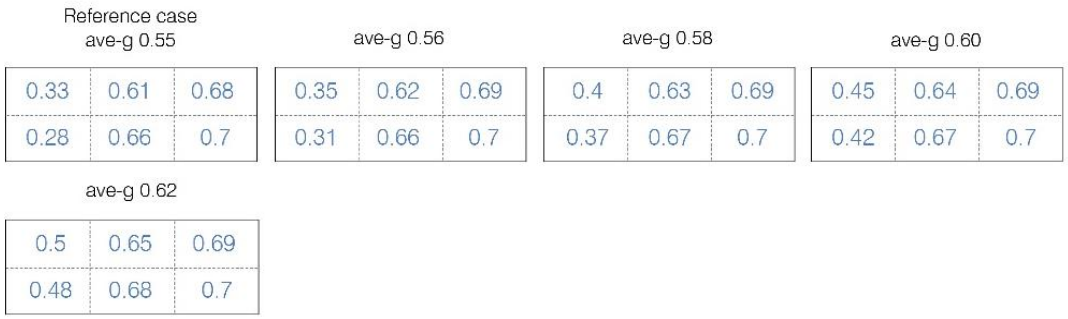

*Figure 63: Ray tracing module output of re-distributed g-*value *for cases with average g-*value *of: 0.55 (Reference Case), 0.56, 0.58, 0.60, and 0.62.*

6.2.12.2 Data output

Table 17 shows the number of hours (annually) above each threshold temperature before (uni-g) and after (ave-g) applying the method to the comfort analysis in Point 0 for selected average g-values of the facade.

*Table 17: Number of hours with $T_{o,Adj}$ > 26, 28, 30 and 35°C for cases with average g-*value *of: 0.55 (Reference Case),0.56, 0.57, 0.58, 0.59, 0.60, 0.61, 0.62, 0.63.*

	uni-g 0.55 (RefCase) /h	ave-g 0.55 (RefCase) /h	ave-g 0.56 /h	ave-g 0.58 /h	ave-g 0.60 /h	ave-g 0.62 /h
≥26 °C	1110	1015	1061	1113	1144	1204
≥28 °C	655	530	583	632	671	754
≥30 °C	409	279	329	370	400	448
≥35 °C	128	17	36	64	96	123

The results in *Figure 64* show that, depending on which threshold temperature the client asks for, the average *g*-value of the façade can be increased. For the Reference case, the average *g*-value can be increased from 0.55 to 0.59 (distributed *g*-value) and still maintain the performance of the uniform *g*-value 0.55 scenario.

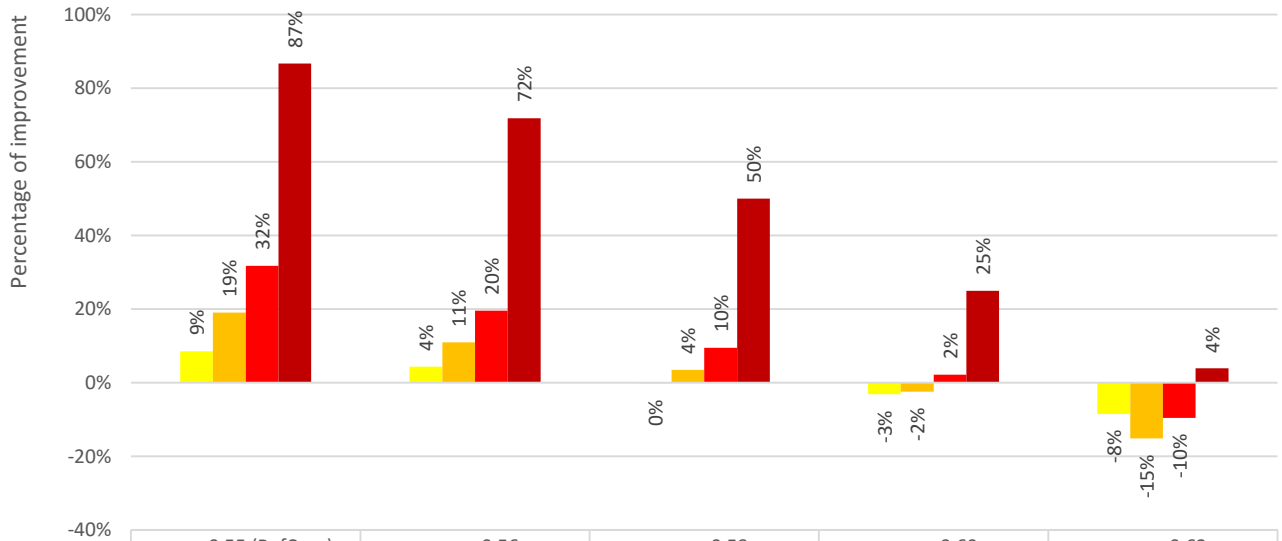

	ave g 0.55 (RefCase)	ave g 0.56	ave g 0.58	ave g 0.60	ave g 0.62
≥26 °C	9%	4%	0%	-3%	-8%
≥28 °C	19%	11%	4%	-2%	-15%
≥30 °C	32%	20%	10%	2%	-10%
≥35 °C	87%	72%	50%	25%	4%

*Figure 64: Difference in number of hours with $T_{o,Adj}$ > 26, 28, 30 and 35°C for cases with average g-*value *of: 0.55 (Reference case),0.56, 0.58 , 0.60, 0.62 for Copenhagen climate.*

7 Analysis/Discussion

The relation between thermal comfort and average *g*-value is the basis upon which this thesis has evolved. The complexity of this relationship has revealed itself through several pursuits of trial and error, gradually shaping an understanding of the impacts of the proposed Shade-tracing tool's limitations and potential to influence design.

A limitation of applying only simple window indices to thermal exchange calculations is that the *g*-value assigned to the glass represents the shading coefficient at normal incidence. Normal incidence however, is a rare occurrence in building simulations since the majority of incoming rays have a high angle of incidence. The absolute consequence of this simplification on the results of this study is unknown. However, one could presume that heat gains through glass with non-angular *g*-values, as assumed to be the case in this study, may, at times of high solar incidence angles, be misestimated.

A fundamental assumption of this study is that the average *g*-value of a glazing unit is equivalent to an equally sized glazing unit with a higher *g*-value, combined with an area of opaque frit corresponding to the difference in *g*-value. This assumption accounts for thermal effects of adding frit to the exterior of a single pane window and does not consider physical complexities of more advanced glazing systems. Hereby, a potential source of error is introduced when applying the shade-tracing methodology to more advanced glazing systems.

Another central assumption of the methodology, is how the method values the direct solar component's influence on thermal discomfort. Does the shading need for a point vary, relative the magnitude of the direct solar component on the point and if so, how? Since the physical relation of these parameters were not known, a simplification, assuming a linear correlation, was made.

A linear weighing factor between 0 and 1 was assigned to all "problematic intersections" on the façade with a high relative solar component, in order to declare the relative comfort deterioration of each intersection. The factor is derived from the difference between measured mean radiant (MRT) and adjusted operative temperature ($T_{op,Adj}$), delta T, in a point at a certain hour, where the maximum delta T for the analysis period is assigned a factor 1. Since delta T is an absolute value, the weighing factor does not differentiate between if delta T is for example the difference between 26°C and 36°C or the difference between 36°C and 46 °C. Hereby, the factor does not include the real thermal influence of delta T, creating an unknown source of error. One could expect, that the relative impact of the factor should increase as the influence of MRT increases. Additionally, the factor does not consider the influence of duration of overheating, for which there is no understanding of whether four hours of 30°C is better or worse than three hours of 40°C, a correlation which requires in depth understanding of human discomfort and tolerance. Theory connecting comfort to for example productivity could be incorporated into the method, to expand the influence of time on discomfort further in the method. Nevertheless, the linear weighing factor seems to correspond to the trends of significant overheating in this project, which suggests that the relation may be an adequate simplification.

To validate the functionality of the simulation tool, a comprehensive Reference Case was essential. The input settings, in particular with regards to parameters enhancing initial overheating problems, prove to be of outmost importance to the favorability of the tool. Such parameters include; thermal transmittance of the envelope (both *g*-value and *U*-value), glazing to floor ratio, ventilation set point temperatures and climate conditions.

Another clear result is how the efficiency of the tool decreases with increased analysis area. As expected, by increasing the analyzed area (number of analysis points), the precision of the tool is diluted, since the redistributed *g*-value is spread over a larger area on the façade. Correspondingly, the tool shows greater efficiency with diminishing façade grid size, since the precision of the problematic region of the façade increase. Secondary effects of increasing the precision of analysis points and façade grid size, are the altered and potentially decreased comfort levels in other parts of the space. When the *g*-value is redistributed with preference to a defined/specific area, remaining areas in the space may be exposed to direct and indirect effects of increased solar loads including increased internal reflection and heat storage etc.

Time distribution results of changing the Reference Case orientation, indicate, as expected, that the tool reduces morning and afternoon peaks from and easterly and westerly direction respectively. The magnitude of these time specific reductions correlate strongly to the cloud coverage at the time of comparison. However, rather unexpectedly, the tool proves to reduce peaks even with higher cloud coverage during the same period, providing reason to believe that there may be an influence of diffuse radiation.

Since annual results are not always of outmost relevance for shading need, the analysis period was shortened. Seasonal simulations, performed for the summer season, was the most beneficial for the indoor comfort. Generally, it can be observed that shorter analysis periods prove more efficient for the tool. In this case, the summer season proves most efficient since this period is most problematic for overheating in the analyzed zone.

If a designer has a requirement of maximum overheating hours above a certain threshold temperature, which is common comfort regulation in Sweden, the tool is able to inform if and how much an average distributed *g*-value can be increased in order not to override certain threshold temperatures. The tool is hereby able to indicate a saving potential to the user of the method. For the Reference Case in this study, the average *g*-value of the glazed façade could be increased from 0.55 to 0.62 without exceeding the initial hours above 35°C. The potential increase in average *g*-value could correspond to economic savings by being able to install cheaper glazing units (with less solar control), energy savings by reducing local peak temperatures, and increase the wellbeing of occupants by elevating daylight levels and clear views to the outside. Furthermore, variations in light and heat transmission through a façade may have positive impacts on occupants' and perhaps encourage physiological adaptation

Overall, the results from the sensitivity analyses are case specific, and can therefore not guarantee comparable outputs for other cases. However, the results from the sensitivity study coincide in three main conclusions for the tool; 1. The more defined the location of the overheating problem is, the greater the efficiency of the method, 2. The more excessive the initial overheating problem is, the lesser the value of the method and 3. The method successfully eliminates peak temperatures to a greater extent in all observed cases.

Without significant deviation, the correlation of results within these main conclusions give reasons to justify the reliability and purpose of the developed methodology, namely to inform designer of the potential to improve local thermal comfort with the shade-tracing tool.

8 Conclusion

A methodology has been developed to correlate overheating with shading need. The method gives numerous visual and numerical output, informing designers of how to distribute the *g*-value of glazed façades in order to mitigate local discomfort to the extent possible with static shading design. The methodology has been developed into a design tool, scripted in Rhino/Grasshopper, enabling parametric applicability. The general conclusions, drawn from the analysis of the results are stated below:

- Thermal discomfort due to solar gains in highly glazed spaces, can be improved by redistributing *g*-values of the glazing according to this method.
- Regions of a façade source to problematic solar gains, can be clearly defined both numerically and visually on a geometric model, for which accurate portrayal of local shading need is easily attainable.
- The usefulness of the method is dependent upon the extent of the initial overheating problem, showing greater effectiveness for lower glazing ratios, lower average *g*-values and cooling set points respectively.
- For all parameters, the method is more effective at reducing higher temperature peaks.
- The more defined the analysis area of floor and the grid on the façade, the higher the effectiveness of the method.
- The method shows considerable improvements for overheating in glazed spaces in moderate climates with high solar radiation. The method becomes less effective for glazed spaces in very hot climates.
- Cloud coverage impacts the effectiveness considerably.

More specific conclusions regarding “shoe box” Reference Case located in Copenhagen are summarized below:

- The method works differently depending on orientation, showing considerable improvements for an East facing glazed façade.
- The method works most efficiently for a seasonal analysis period.

More specific conclusions regarding the tool are summarized below:

- Tool enables parametric design.
- No geometric limitations, cases with numerous glazing surfaces, analysis points and surrounding context can be evaluated with the tool.
- The method gives simple means of comparative analysis, useful for weighing alternatives against each other.

8.1 Future work

The following aspects are considered necessary for further development of the methodology of the shade-tracing tool.

1. Evaluate the relation of advanced glazing types/systems and frit.
2. The actual impact of degree hours on shading need (*g*-value). i.e. explore the limitations of the linear factoring/weighing method developed in this thesis. Potentially correlate to economic factors such as productivity (loss) of occupants.
3. Evaluate the secondary effects of distributing *g*-value with regard to increasing discomfort in points/areas not analyzed by the tool.
4. Study the impact of angular *g*-value with detailed glazing definitions in EnergyPlus
5. Although diffuse radiation is included in the weather files, the influence of diffuse solar component on comfort levels is not accounted for in this method. The influence of the diffuse component should be analyzed further.
6. Explore the tools functionality on complex cases for example to establish appropriate situations for the tool to be used successfully. i.e climates, building types, occupancy, construction details, HVAC capacities, regulations etc.
7. Verify the tool with physical measurements
8. Consider the impact on visual comfort
9. Other shading types than frit, varying opacity and adaptability

10. Reverse the outcome of the tool, Glazing need = 1-shading need
11. Further develop the linear correlation between shading need and thermal discomfort due to direct solar component assumed in this project.

7 References

AGC, 2013. *AGC Glass Pocket Guide.* s.l.:s.n.

ANSI/ASHRAE Standard 55, 2010. *Thermal Environmental Conditions for Human Occupancy,* s.l.: s.n.

Arens & Hoyt & Zhou, 2015. *Modeling the comfort effects of short-wave solar radiation indoors.,* s.l.: Center for the Built Environment UC Berkeley.

Athienitis, A. & Santamouri, M., 2013. *Thermal Analysis and Design of Passive Solar Buildings.* New York: Earthscan from Routledge.

Blomsterberg & Dalman & Gräslund & Henriksson & Jansson & Jonsson & Kellner & Levin & Sjögren, 2013. *Brukarindata kontor,* s.l.: Sveby.

Blomsterberg, Å., 2007. *KONTORSBYGGNAD I GLAS,* Malmo: s.n.

Bojic, M., 2013. *Optimization of thermal comfort in buildings through envelope design,* s.l.: s.n.

Brager, G. & de Dear, R., 2001. *Climate, Comfort, & Natural Ventilation: A new adaptive comfort standard for ASHRAE Standard 55.* s.l., s.n.

Byggestyrelsen, E.-. o., 2014. *Bygningsreglementet 2010,* s.l.: s.n.

Cengel Y. A., G. A. J., 2011. *Heat and Mass Transfer: Fundamentals & Applications.* s.l.:McGraw-Hill.

CIBSE, 2006. *Environmental design. CIBSE Guide A.*. London: Page Bros. (Norwich) Ltd..

de Dear & Brager & Cooper, 1997. *Developing a Model for Adaptive Thermal Comfort and Preference.* s.l., s.n.

EnergyPlus, 2015. *https://energyplus.net/.* [Online]
[Accessed 1 Septemeber 2015].

Evans, B., 2015. *Overheating in homes. Keeping a growing population cool in summer.*. London: WSP/ Parsons Brinckerhoff.

Folkhälsomyndigheten, 2014. *Folkhälsomyndighetens allmänna råd om tempertatur inomhus, FoHMFS 2014:17,* s.l.: s.n.

grasshopper3d, 2015. *www.grasshopper3d.com.* [Online]
[Accessed 1 September 2015].

Griffith & Arasteh & Kohler, 2009. *Modeling Windows in Energy Plus with Simple Perfomance Indices,* Berkeley: Lawrence Berkeley National Laboratory.

Hacker, N. & Holmes, M., 2007. *Energy and Buildings. Climate change, thermal comfort and energy: Meeting the design challenges of the 21st century.,* London: Arup.

Huizenga & Zhang & Mattelaer & Yu & Arens & Lyons, 2006. *Window Performance for Human Thermal Comfort,* s.l.: s.n.

ISO, 2005. *ISO 7730:2005(E). Ergonomics of the thermal environment.,* s.l.: ISO copyright office.

Lang, B., n.d. *Energy Implications for Glass.* s.l.:www.LiveGlass.com.

Lyons & Arasteh & Huizenga, 1999. *Window Performance for Human Comfort,* s.l.: s.n.

Mackey, C., 2015. *Pan Climatic Humans - Shaping Thermal Habits in an Unconditioned Society,* Massachusetts: Massachusetts Institute of Technology.

McCluney, R., 2002. *Methods for determining the SHGC of Complex fenestration.*. Florida: Methods for determining the SHGC of Complex fenestration.

Persson, M.-L., 2006. *Windows of Opportunities,* Uppsala: Uppsala University.

Poirazis, H., 2008. *Single and Double Skin Glazed Office Buildings.* Lund: LTH.

Radiance, 2015. *http://www.radiance-online.org/about/main.html.* [Online]
[Accessed 1 September 2015].

Rosenfeld, J., 1996. *On the calculation of the total solar energy transmittance of complex glazings.,* s.l.: University of Wales.

Roudsari, M., 2015. [Online]
Available at: https://mostapharoudsari.gitbooks.io/honeybee-primer/content/text/components/Set_EnergyPlus_Zone_Thresholds.html
[Accessed 1 September 2015].

Roudsari, M., 2015.
https://github.com/mostaphaRoudsari/ladybug/blob/master/src/Ladybug_Import%20epw.py.
[Online]
[Accessed 1 September 2015].
Sargent & Niemasz & Reinhart, 2011. *Shaderade: Combining Rhinoceros and EnergyPlus for the design of static exterior shading devices.* Cambridge, Harvard University Graduate School of Design.
Schittich & Sobek & Staib & Balkow & Schuler, 2007. *Glass Construction Manual, Edition Detail.* s.l.:Walter de Gruyter.
Standards, B., 2011. *Glass in Building. DEtermination of luminous and Solar Characteristics of Glazing,* s.l.: BSI Standards.
Strange, V. N., 2015. *Vindues- og Facadedag 2015, Orientering om BR2015 og 2020,* s.l.: s.n.
Taffe, P., 1997. A Qualitative Respons Model of Thermal Comfort. *Building and Environment,* Vol. 32(No. 2), pp. pp. 115-121.
Wall, M., 1996. *Climate and Energy Use in Glazed Spaces.* Lund: Wallin & Dalholm Boktryckeri AB.

8 Appendix

The thermal module was structured as follows.

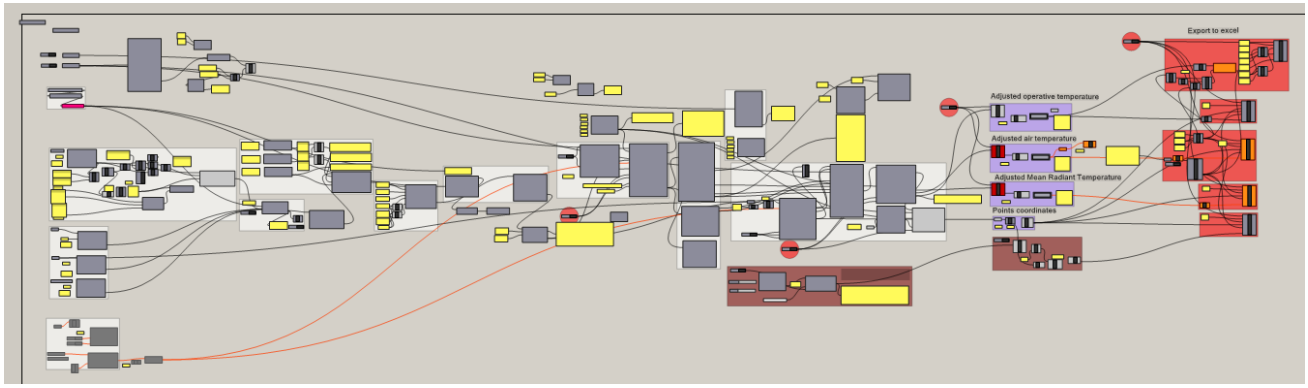

The shade-tracing tool was defined as follows

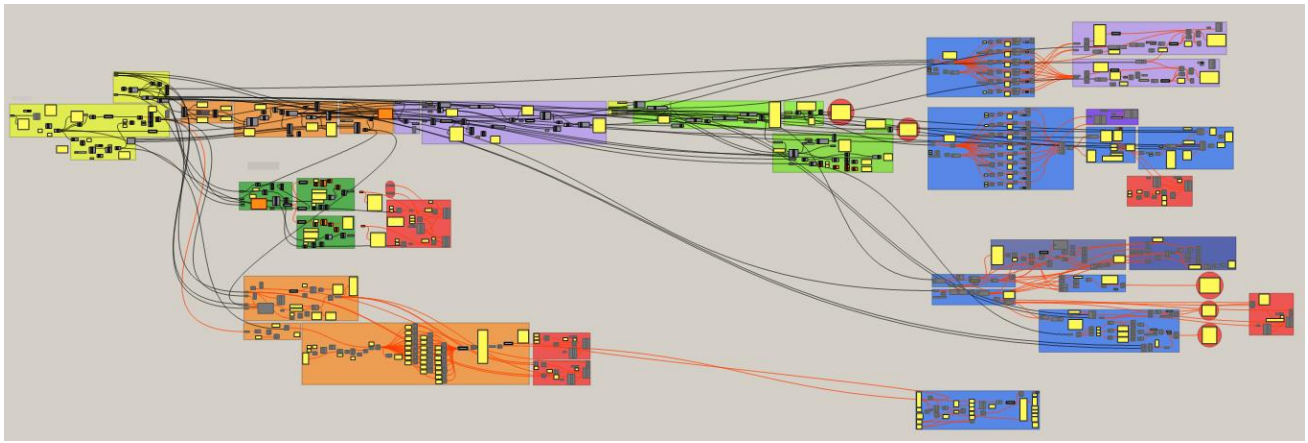

LUND UNIVERSITY

Dept of Architecture and Built Environment: Division of Energy and Building Design
Dept of Building and Environmental Technology: Divisions of Building Physics and Building Services%